Heat Shock Factor Regulation of Antimicrobial Peptides Expression Suggests a Conserved Defense Mechanism Induced by Febrile Temperature in Arthropods

Bang Xiao [1, 2], Shihan Chen [1, 2], Yue Wang [1, 2], Xuzheng Liao [1, 2], Jianguo He [1, 2, 3, *], Chaozheng Li [1, 2, 3, **]

1. School of Marine Sciences, Sun Yat-sen University, State Key Laboratory of Biocontrol /Southern Marine Science and Engineering Guangdong Laboratory (Zhuhai), Guangzhou, P. R. China

2. Guangdong Provincial Key Laboratory of Marine Resources and Coastal Engineering/ Guangdong Provincial Key Laboratory for Aquatic Economic Animals, School of Life Sciences, Sun Yat-sen University, Guangzhou, P. R. China

3. China-ASEAN Belt and Road Joint Laboratory on Mariculture Technology, Guangzhou, P. R. China

**, Corresponding Author:
Chaozheng Li, Ph.D.
School of Marine Sciences
Sun Yat-sen University
Guangzhou, 510275
P. R. China
Email: lichaozh@mail2.sysu.edu.cn

*, Corresponding Author:
Jianguo He, Ph.D.
School of Life Sciences
Sun Yat-sen University
Guangzhou, 510275
P. R. China
Email: lsshjg@mail.sysu.edu.cn

Abstract:

Temperature is a critical factor influencing the outbreak and progression of viral diseases in organisms. Febrile temperatures have been shown to enhance immune competence and reduce viral replication in various species. However, the underlying mechanisms remain largely unknown. In this study, we investigate the molecular mechanisms by which elevated temperatures confer resistance to viral infections, focusing on the role of heat shock factor 1 (HSF1) in regulating antimicrobial effectors rather than the traditional target genes molecular chaperones. Using shrimp *Litopenaeus vannamei* as a model, we demonstrate that febrile temperatures induce HSF1, which in turn upregulates antimicrobial peptides (AMPs) that target viral envelope proteins and inhibit viral replication. Importantly, this is the first to show that HSF1 directly binds to the heat shock elements (HSE) motifs of AMPs both in shrimp and *Drosophila* S2 cells, suggesting this may be a conserved regulatory mechanism in arthropods. Additionally, our findings highlight the role of HSF1 beyond the classical heat shock response, revealing its critical function in modulating innate immunity. These insights provide new avenues for managing viral infections in aquaculture and other settings by leveraging environmental temperature control.

Keywords: Temperature; Innate immunity; Virus; Heat shock factor (HSF); Antimicrobial peptides (AMPs)

1. Introduction

The proliferation of pathogens and the outbreak of diseases are influenced by various factors, including transmission vectors, host species, and environmental conditions (Marcogliese, 2008). Among these, temperature is one of the most critical environmental factors, significantly impacting disease occurrence and prevalence (Hou et al., 2023). Temperature can directly affect the immune response, metabolism, feeding rate, oxygen consumption, growth, and survival of animals (Deldicq et al., 2021). Aquatic animals such as fish, shrimp, crabs, and shellfish are ectothermic, and their susceptibility to diseases is directly related to temperature (Marcogliese, 2008). In fishes, Koi herpesvirus (KHV) can cause massive mortality in carp and koi carp at temperatures between 23-28 °C, while temperatures above 30 °C typically do not result in mortality (Yuasa et al., 2008). In crustaceans, high temperatures (32-33 °C) have been demonstrated to inhibit white spot syndrome virus (WSSV) replication and reduce mortality in infected shrimp (Du et al., 2006; Guan et al., 2003; Jiravanichpaisal et al., 2004). Notably, many ectothermic animals can respond to exogenous pathogenic infections by seeking warmer external environments (Covert and Reynolds, 1977; Louis et al., 1986). When infected, some ectothermic animals such as fish, insects, and crustaceans elevate their body temperature by moving to warmer areas (Bundey et al., 2003; Rakhshaninejad et al., 2023; Rakus et al., 2017). This behavioral fever, similar to fever responses in higher organisms, can help hosts suppress or overcome infections (Hasday et al., 2014), although the mechanisms underlying this heat-induced antimicrobial immunity remain unclear.

The heat shock response (HSR), also known as the heat stress response, serves as a bridge linking elevated temperatures with increased immunity (Tian et al., 2021). The HSR induced by temperature increase primarily involves the expression of heat shock proteins (HSPs) and other related factors regulated by heat shock transcription factors (HSFs) (Lang et al., 2021). Under non-stress conditions, HSF monomers are retained in the cytoplasm in a complex with HSP90 or the cytosolic chaperonin TCP1 ring complex (TRiC) (Neef et al., 2014). During the stress response, HSF dissociates from the complex, trimerizes, and converts into a DNA-binding conformation (Zheng et al.,

2016). Activated HSF induces gene transcription through regulatory upstream promoter elements known as heat shock elements (HSEs) (Andrasi et al., 2021). In the face of thermal or pathogenic stress, the heat shock response functions as a highly conserved cellular mechanism across various organisms (Anckar and Sistonen, 2011). Research suggests that the HSF-mediated heat shock response plays a crucial role in the regulation of the innate immune network through a combination of direct gene regulation, interaction with immune signaling pathways, and the broader cellular stress response (Morimoto, 2011). In *Drosophila*, HSF-deficient flies, lacking a heat shock response, exhibit high sensitivity to viral infection (Merkling et al., 2015), indicating that the heat shock response is a crucial component of innate antiviral immunity.

Heat shock factors (HSFs) are primarily recognized as inducible transcriptional regulators of genes encoding molecular chaperones and other stress proteins (Akerfelt et al., 2010). Interestingly, members of the HSF family also participate in various cellular processes, including apoptosis, the unfolded protein response (UPR), oxidative stress, multidrug resistance, and pathogenic infection (Anckar and Sistonen, 2011). Consequently, the repertoire of HSF targets has expanded well beyond traditional heat shock genes (Barna et al., 2018). Recent research has illuminated the interplay between the heat shock response (HSR) and the innate immune system, revealing that HSFs can regulate innate immune responses (Akerfelt et al., 2007). For instance, HSF1, the primary HSF, can modulate the expression of pro-inflammatory cytokines such as TNF-α, IL-1β, and IL-6, thereby influencing the inflammatory response (Barna et al., 2018). Additionally, HSF1 has been shown to interact with and influence the activity of the NF-κB and MAPK pathways, thus altering the cellular environment to modulate the innate immune response (Chen et al., 2010). These unexpected observations indicate complexity of HSF function. At present, however, the mechanisms by which the HSF family affects innate immunity are still poorly understood.

To explore the underlying mechanisms of the febrile temperature-inducible HSF in host antiviral immunity, the shrimp *Litopenaeus vannamei* was challenged with WSSV, and the thermal regulation of host immunity was characterized. The results indicated that febrile temperature-inducible HSF1 confers virus resistance by regulating

115 the expression of antimicrobial peptides (AMPs) in *L. vannamei*. Additionally, it was
116 revealed that high temperature (30 ℃) restricts the replication of *Drosophila* C virus
117 (DCV) in an invertebrate model system (*Drosophila* S2 cells) also mediated by the
118 HSF1-AMPs axis. Together, these results suggest that heat shock factor regulation of
119 AMPs expression is a conserved defense mechanism induced by febrile temperature in
120 arthropods.

2. Results

2.1 Induction of Heat Shock Factor 1 at High Temperature (32 °C)

Studies have demonstrated that high temperatures (above 30 °C) markedly reduce mortality in shrimp infected with WSSV, while temperatures ranging from 22 to 30 °C favor higher levels of WSSV replication and associated mortality (Lin et al., 2011; Rahman et al., 2007; Xiao et al., 2024). To uncover the molecular mechanisms by which high temperature restricts WSSV infection, RNA-seq was performed to identify genes responsive to high temperature, particularly those encoding potential transcriptional regulators. Two shrimp groups, Group TW and Group W, were cultured at 25 °C. Group W comprised shrimp injected with WSSV and maintained at 25 °C continuously. In contrast, Group TW was subjected to a temperature increase to 32 °C at 24 hours post-injection (hpi). Gill samples were collected for analysis 12 hours post-temperature rise (hptr) and subjected to Illumina sequencing (Fig. 1A). As shown in Fig. 1B and 1C, 10 of the 1285 high temperature-induced genes were predicted to encode transcription factors.

GO functional enrichment analysis of DEGs between group TW and group W, indicating that most DEGs were involved in biological processes such as protein refolding, chaperone-mediated protein folding, and heat response (Xiao et al., 2024). Special attention has been paid to heat shock factor 1 (HSF1), the master regulator of the heat shock response, which upon activation induces not only classical heat shock genes but also a broad array of genes beyond the scope of molecular chaperones (Barna et al., 2018). To validate the high-throughput sequencing results, the expression profile of these transcription factors was confirmed by qPCR, showing a significant increase in *Litopenaeus vannamei* HSF1 (LvHSF1) expression (Supplementary Fig. 1). These results suggest that LvHSF1 may play a potential role in enhancing shrimp resistance to WSSV at elevated temperatures (32 °C).

2.2 Expression Profiles of LvHSF1 in Shrimp Under Varied Temperature Conditions and WSSV Challenge

To determine that LvHSF1 is related to high temperature and WSSV infection, its expression level was measured under high temperature and after WSSV infection. Tissue distribution analysis showed that LvHSF1 was expressed in all examined tissues at room temperature (25 °C) and increased rapidly in all tested tissues at high temperature (32 °C; Fig. 2A). Additionally, the protein expression of LvHSF1 was significantly up-regulated in hemocytes, gills, and intestines when exposed to 32 °C (Fig. 2B). Next, we detected the expression of LvHSF1 in the immune response to Poly (I:C) and WSSV at 25 °C. Following exposure to Poly (I:C) at 25 °C, LvHSF1 expression was upregulated at 12 h (2.43-fold), 24 h (2.60-fold), and 36 h (4.33-fold) in hemocytes (Supplementary Figure 2A); slightly upregulated at 4 h (1.97-fold) and downregulated at 12 h (0.64-fold) in gills (Supplementary Figure 2B); and slightly downregulated at 4 h (0.41-fold) and upregulated at 8 h (1.15-fold) in intestines (Supplementary Figure 2C). In response to WSSV infection at 25 °C, LvHSF1 expression in hemocytes was dramatically induced, peaking at 8 hours (6.04-fold; Supplementary Figure 2D). In the gills, LvHSF1 expression initially increased at 8 hours (2.10-fold) and significantly again at 72 hours (2.80-fold; Supplementary Figure 2E). In the intestines, a marked induction of LvHSF1 was observed at 8 hours (2.23-fold; Supplementary Figure 2F).

Further investigation revealed LvHSF1's role in the immune response to Poly (I:C) and WSSV at 32 °C. Following exposure to Poly (I:C) at 32 °C, LvHSF1 expression was upregulated at 4 h (5.68-fold), 12 h (8.44-fold), and 24 h (7.52-fold) in hemocytes (Fig. 2C); strongly induced at 24 h (7.00-fold) in gills (Fig. 2D); and slightly upregulated at 8 h (3.47-fold) and 14 h (2.60-fold) in intestines (Fig. 2E). In response to WSSV infection at 32 °C, LvHSF1 expression in hemocytes was dramatically induced, peaking at 36 hours (15.93-fold; Fig. 2F). In the gills, LvHSF1 expression initially increased at 8 hours (3.9.-fold) and significantly again at 48 hours (4.56-fold; Fig. 2G). In the intestines, the expression level of HSF1 remained at a high level from 8 to 48 hours (3.20~4.17-fold; Fig. 2H). These results suggest that LvHSF1 is actively involved in the response to low (25 °C) and high (32 °C) temperature, and viral (WSSV) infection.

180

181 **2.3 Role of LvHSF1 in Restricting WSSV at Low (25 °C) and High (32 °C)**
182 **Temperatures**

183 To investigate LvHSF1's role in shrimp during WSSV infection, RNA interference
184 (RNAi) was employed *in vivo*. Two double-stranded LvHSF1 (dsLvHSF1) constructs
185 were synthesized: dsLvHSF1-1 (targeting 443-1001 bp) and dsLvHSF1-2 (targeting
186 1365-1854 bp). Analysis revealed a significant reduction in both transcription and
187 protein levels of LvHSF1 in hemocytes (Figs. 3A, 3a) and gills (Figs. 3B, 3b), with
188 dsLvHSF1-1 showing greater silencing efficiency. Consequently, dsLvHSF1-1 was
189 selected for subsequent knockdown experiments. After LvHSF1 knockdown, shrimp
190 were challenged with WSSV, and viral titers were quantified using absolute quantitative
191 PCR. Shrimp with silenced LvHSF1 exhibited increased viral loads in hemocytes (Fig.
192 3C) and gills (Fig. 3D) at low temperature (25 °C). Additionally, transcription levels of
193 VP28, one of the major structural proteins of WSSV, were higher in the LvHSF1-
194 silenced group than in the GFP-silenced control in hemocytes (Fig. 3E) and gills (Fig.
195 3F). Similarly, the levels of VP28 protein were significantly elevated in the HSF1-
196 silenced group (Figs. 3G, 3g). However, no significant difference in shrimp survival
197 rates was observed between LvHSF1-silenced shrimp and GFP-silenced shrimp at low
198 temperature (25 °C) ($p = 0.8657$; Fig. 3H).

199 Next, LvHSF1's role in shrimp during WSSV infection at high temperature (32 °C)
200 was further determined. Notably, the survival rate of LvHSF1-silenced shrimp infected
201 with WSSV was significantly lower than the control group at high temperature (32 °C)
202 ($p < 0.001$; Fig. 4A). Shrimp with silenced LvHSF1 exhibited increased viral loads in
203 gills (Fig. 4B) and hemocytes (Fig. 4C) at high temperature (32 °C). Additionally, VP28
204 protein levels were significantly elevated in the LvHSF1-silenced group in gills at high
205 temperature (32 °C; Figs. 4D, 4d). These data suggest that LvHSF1 plays a crucial role
206 in antiviral immunity against WSSV infection especially at high (32 °C) temperatures.

207

208 **2.4 SWD as a Potential Antiviral Effector Regulated by LvHSF1**

To determine how temperature-induced LvHSF1 restricts WSSV infection, RNA-seq was performed to identify target genes regulated by LvHSF1. Candidates whose expression was inhibited by LvHSF1 knockdown after WSSV infection at high temperature (32 °C) were screened. As shown in Fig. 5A and 5B, 8 of the 954 dsHSF1-suppressed genes were predicted to encode effector factors. These differentially expressed genes (DEGs) included immunity-effector molecules, such as heat shock proteins, antimicrobial peptides and cytokines, and the classical heat shock proteins were downregulated by the RNA-seq (Supplementary table 2). Among the 8 candidate genes, the anti-WSSV role of C-type lectins (CTLs), Anti-lipopolysaccharide factor (ALF) and Vago have been proved in shrimp (Gao et al., 2021; Methatham et al., 2017; Zhao et al., 2009). Therefore, particular attention was paid to the **n**ewly identified **s**ingle **w**hey acidic protein **d**omain-containing protein, designated SWD. The SWD belongs to type III crustins, which are crustacean cationic cysteine-rich antimicrobial peptides containing one or two whey acidic protein (WAP) domains at the carboxyl terminus and mainly exert antimicrobial activities (Supplementary Fig. 3). The detailed regulatory mechanism of SWD against WSSV was unclear. To validate the high-throughput sequencing results, the expression level of SWD and effector molecules were confirmed by qPCR, showing a significant reduction in hemocytes and gills after LvHSF1-knockdown (Fig. 5C; Supplementary Fig. 4). These results suggest that SWD may play a pivotal role against WSSV infection regulated by LvHSF1.

To determine whether LvHSF1 regulates the expression of SWD *in vitro*, a dual-luciferase reporter assay was performed in *Drosophila* S2 cells. The promoter region of SWD was cloned by genome walking, containing two putative conserved HSE motifs located at approximately −1371 to −1359 (HSE-1) and −1035 to −1023 (HSE-2; Supplementary table 3). The dual-luciferase reporter assay showed that the promoter of SWD could be regulated by ectopic expression of LvHSF1 in a dose-dependent manner (Figs. 5D and 5d). Three reporter plasmids containing mutant promoter regions of SWD with one or no HSE motifs were constructed, named pGL3-SWD-M1, pGL3-SWD-M2, and pGL3-SWD-M1/2, respectively (Fig. 5E). The reporter assay results showed that the ectopic expression of LvHSF1 could also improve the promoter activity of pGL3-

239 SWD-M1 and pGL3-SWD-M2, whereas the activity of pGL3-SWD-M1/2 was not
240 upregulated (Figs. 5F and 5f), suggesting that putative HSE binding motifs play
241 significant roles in LvHSF1-mediated SWD induction.

242 To further confirm this, EMSA experiments were performed to investigate the
243 direct interaction between LvHSF1 and HSE motifs of SWD. Biotin-labeled probes or
244 mutant probes of the HSE motifs were synthesized (Fig. 5G). LvHSF1 protein was
245 purified to verify its ability to bind to the HSE motifs (Supplementary Figs. 5A and 5B).
246 The results showed that band shifts of protein-DNA complexes were detected when
247 LvHSF1 protein was incubated with biotin-labeled probe1 but not mutant biotin-labeled
248 probe1 (Fig. 5H). Additionally, the band shifts could be competitively reduced when
249 LvHSF1 protein was incubated with wide-type unbiotinylated probe1 at 20- and 100-
250 fold molar excess (Fig. 5H). A similar result was observed in the interaction between
251 LvHSF1 protein and the biotin-labeled probe2 (Fig. 5H). No band shift was observed
252 in the control set (GST), suggesting that the interaction between LvHSF1 protein and
253 each of the HSE binding motifs is specific. Moreover, the recombinant protein HSF1
254 could significantly induced the expression level of SWD in shrimp (Supplementary Fig.
255 5C). These results strongly demonstrate that LvHSF1 could regulate the expression of
256 SWD *in vitro* and *in vivo*.

257

258 **2.5 SWD Inhibits WSSV Replication and Interacts with WSSV Envelope Proteins**

259 To confirm whether SWD is involved in WSSV infection, qPCR was performed to
260 determine the expression profile of SWD. When shrimp were infected with WSSV, the
261 expression of SWD was upregulated at 4 h (5.66-fold) and 12 h (5.60-fold), remained
262 high at 36 h (5.18-fold) and 48 h (7.90-fold), and slightly downregulated at 72 h (4.74-
263 fold; Fig. 6A). To reveal the role of SWD in WSSV infection at high temperature
264 (32 °C), RNA interference (RNAi) was performed to knock down SWD expression.
265 The mRNA level of SWD was effectively suppressed by specific dsSWD in gills, and
266 the value was downregulated to 0.30-fold of the dsGFP (green fluorescent protein)
267 injection group (as a control) (Fig. 6B). The viral load of the dsSWD group was
268 considerably higher than the control group (Fig. 6C). Additionally, the survival rate of

269 shrimp in the SWD-silenced group was significantly lower than in the GFP-knockdown
270 group ($p < 0.01$; Fig. 6D).

271 To further demonstrate the actual role of SWD *in vivo*, RNAi experiments coupled
272 with rSWD proteins injection were performed. Recombinant proteins of rSWD and
273 rTrx-His-tag were expressed, purified by Ni-NTA resin, and confirmed by Coomassie
274 staining (Fig. 6E), and the results were further confirmed by Western blot analysis (Fig.
275 6F). After knockdown of endogenous SWD, shrimp samples were treated with WSSV
276 mixed with rSWD or rTrx-His-tag by intramuscular injection at high temperature
277 (32 °C). Consequently, the viral load of those co-injected with rSWD was significantly
278 reduced compared to the control group ($p < 0.01$; Fig. 6G). Additionally, the survival
279 rates of shrimp co-injected with rSWD were significantly higher than the control group
280 ($p < 0.01$; Fig. 6H). Therefore, SWD plays a crucial role in the immune defense against
281 WSSV infection at high temperature (32 °C) *in vivo*.

282 Next, to verify whether the anti-WSSV function of SWD was regulated by LvHSF1
283 at high temperature (32 °C), *in vivo* RNAi-LvHSF1 experiments coupled with rSWD
284 injection were performed. After knockdown of LvHSF1, shrimp samples were treated
285 with WSSV mixed with rSWD or rTrx-His-tag by intramuscular injection at high
286 temperature (32 °C). The results showed that the viral load of those co-injected with
287 rSWD was significantly reduced compared to the control group ($p < 0.01$; Fig. 6I).
288 Additionally, VP28 protein levels of those co-injected with rSWD were significantly
289 decreased (Fig. 6J, 6j). The survival rates of shrimp co-injected with rSWD were
290 significantly higher than the control group ($p < 0.01$; Fig. 6K). Moreover, after
291 knockdown of SWD, shrimp were injection with rLvHSF1 mixed with WSSV. The
292 results showed that the viral load was significantly lower than the control group 48
293 hours post WSSV infection at high temperature (32 °C) (Supplementary Fig. 5D).
294 Taken together, these results suggest that the anti-WSSV function of SWD at high
295 temperature (32 °C) is mediated by LvHSF1.

296 To reveal the possible anti-WSSV mechanism of SWD, pull-down assays were
297 performed to detect whether rSWD protein could interact with WSSV envelope proteins.
298 The main envelope proteins of WSSV, including VP19, VP24, VP26, and VP28 with

299 GST-tags, were from a previous study. In the GST-tagged pull-down assays, rSWD
300 could interact with VP24 and VP26 based on SDS-PAGE gels with Coomassie blue
301 staining (Fig. 7A), and the result was further confirmed by Western blot analysis with
302 the 6×His antibody (Fig. 7B). Based on the His-tagged pull-down assays, VP24 and
303 VP26 could precipitate rSWD (Fig. 7C), and this result was further confirmed by
304 Western blot analysis with GST antibody (Fig. 7D). Additionally, confocal analysis
305 confirmed that SWD colocalized with VP24 (Fig. 7E and 7e) and VP26 (Fig. 7F and
306 7f) in *Drosophila* S2 cells. Collectively, these results suggest that SWD could inhibit
307 WSSV replication and bind to VP24 and VP26 of WSSV.
308

309 **2.6 Conservation of the Febrile Temperature-Inducible HSF1-AMPs Axis**
310 **Conferring Virus Resistance in Arthropods**

311 To demonstrate whether HSF1 regulation of antimicrobial peptides is a conserved
312 defense mechanism induced by elevated temperature in arthropods, experiments were
313 performed in an invertebrate model system (*Drosophila* S2 cells). Literature reports
314 that the temperature range for optimal growth of *Drosophila* S2 cells is 25–28 °C, and
315 S2 cells tolerated a normal growth temperature of 30 °C. Therefore, S2 cells were
316 cultured at normal temperature (27 °C) or high temperature (30 °C) with or without
317 DCV infection. The results showed that S2 cells were adherent to the wall and grew
318 well at 27 °C or 30 °C without DCV infection, and the cytopathic signs of S2 cells were
319 milder at 30 °C than the control group at 27 °C when infected with DCV
320 (Supplementary Fig. 6A). Additionally, the mRNA and protein expression of DCV was
321 significantly lower at 30 °C than the control group at 27 °C (Supplementary Fig. 6B
322 and 6C). These results suggest that elevated temperature could restrict the replication
323 of DCV in *Drosophila* S2 cells.

324 To determine whether *Drosophila melanogaster* HSF1 (DmHSF1) is related to
325 high temperature (30 °C) and DCV infection in S2 cells, its expression level was also
326 determined. The results showed that the mRNA expression of DmHSF1 was
327 significantly upregulated 4.53-fold and 6.48-fold at high temperature (30 °C) or
328 infected with DCV, respectively (Fig. 8A). Antimicrobial peptides, especially Attacin

329 A, Cecropins A, Defensin, Metchnikowin, and Drosomycin, have been proven to
330 participate in the innate immunity of *Drosophila* in response to viral infection (Zhu et
331 al., 2013). The expression of DmAMPs were explored in response to high temperature
332 (30 °C) and DCV infection. The results showed that Atta, CecA, and Def were
333 significantly upregulated 5.77-fold, 4.55-fold, and 5.40-fold at high temperature
334 (30 °C), respectively (Fig. 8B). When stimulated by DCV, Atta, CecA, Def, Met, and
335 Drs were remarkably increased 46.84-fold, 123.52-fold, 39.72-fold, 41.14-fold, and
336 241.40-fold, respectively (Fig. 8C). These results suggest that DmAMPs play a crucial
337 role in anti-DCV defense at high temperature (30 °C).

338 Next, DmHSF1's role in *Drosophila* S2 cells during DCV infection at high
339 temperature (30 °C) was investigated. Using the RNAi strategy in S2 cells, it was
340 observed that the transcription levels of DmHSF1 can be downregulated by dsRNA-
341 DmHSF1 with or without DCV infection (Fig. 8D). After DmHSF1 knockdown, the
342 mRNA and protein expression of DCV was significantly higher at 30 °C than the
343 control group (Fig. 8E and 8e). Additionally, Atta, CecA, and Def were significantly
344 downregulated 0.65-fold, 0.43-fold, and 0.56-fold in DmHSF1 silenced, DCV infected
345 S2 cells at high temperature (30 °C), respectively (Fig. 8F). Furthermore, S2 cells were
346 transfected with pAc5.1a-DmHSF1-HA or pAc5.1a-HA plasmid (as control;
347 Supplementary Fig. 7A). The results showed that the mRNA and protein expression of
348 DCV was significantly lower at 30 °C than the control group (Fig. 8G and 8g).
349 Accordingly, Atta, CecA, and Def were significantly upregulated 4.38-fold, 1.89-fold,
350 and 3.13-fold at high temperature (30 °C), respectively (Fig. 8H). These results show
351 that high temperature (30 °C) and DCV could induce the expression of DmHSF1 and
352 DmAMPs, with DmHSF1 playing crucial roles in defending against DCV at elevated
353 temperatures. To further verify whether DmHSF1 exerts its anti-DCV function by
354 regulating DmAMPs at high temperature (30 °C), the regulatory roles of DmHSF1 on
355 DmAMPs were investigated through ectopic expression of DmHSF1 and knockdown
356 of DmAMPs during infection. Firstly, the promoter region of DmAtta, DmCecA, and
357 DmDef was cloned, each containing three conserved HSE motifs (Fig. 8I). Dual-
358 luciferase reporter assays showed that the promoter of DmAtta, DmCecA, and DmDef

359 could be upregulated 12.36-fold, 7.76-fold, and 2.71-fold by DmHSF1, respectively.
360 The mutant HSE motifs promoter of DmAtta, DmCecA, and DmDef could not be
361 regulated by DmHSF1 (Fig. 8J). Further, due to the expression of Attacin A was the
362 highest DmAMPs induced by DmHSF1, to demonstrate that DmHSF1 exerts its anti-
363 DCV function by regulating DmAMPs, DmAtta was chosen as a representative. After
364 knockdown of DmAtta (Supplementary Fig. 7B), S2 cells were transfected with
365 DmHSF1 and then infected with DCV. The results showed that the mRNA and protein
366 expression of DCV was significantly lower at 30 °C than the control group (Fig. 8K
367 and 8k). These results suggest that DmHSF1 exerts its anti-DCV function by regulating
368 DmAMPs at high temperature (30 °C).
369

370 **3. Discussion**

371 Temperature is a key factor regulating various biological activities, and for aquatic
372 ectotherms, it significantly affects growth rates and is also a crucial determinant of viral
373 disease outbreaks (Marcogliese, 2008). Accumulating evidence has indicated that
374 increased temperature enhances immune competence, resistance to infection, and levels
375 of immune mediators under febrile conditions (Evans et al., 2015; Hasday and Singh,
376 2000). High temperatures (32-33 °C) have been shown to inhibit the replication of
377 WSSV and reduce mortality in WSSV-infected shrimp (Sun et al., 2014). Studies have
378 reported that WSSV-infected shrimp reared at high temperatures (above 31 °C) exhibit
379 increased total hemocyte count (THC), phenoloxidase (PO) activity, and apoptotic
380 index (Granja et al., 2003; Wu et al., 2015). However, the mechanism contributing to
381 enhanced pathogen resistance in shrimp at high temperatures remains unclear. In this
382 study, our findings revealed the molecular mechanism through which the HSF-AMPs
383 axis mediates host resistance to viruses induced by febrile temperature. Specifically,
384 AMPs are a newly documented type of effector protein targeted by HSF that mediate
385 the host antiviral response beyond the classical heat shock response.

386 Regulating body temperature, particularly increasing it (fever), is one of the
387 primary defense mechanisms in homeotherms against infections (Hasday et al., 2014).
388 Ectotherms as diverse as reptiles, fish, insects, and crustaceans also raise their core
389 temperature during infection through behavioral regulation, seeking warmer
390 environments—a phenomenon known as behavioral fever (Hasday et al., 2014). This
391 feature, preserved in endothermic mammals and birds, strongly suggests that febrile
392 temperatures confer a survival advantage (Bicego et al., 2007). In 1975, Kluger and
393 colleagues published the first direct experimental study demonstrating the benefits of
394 elevated temperature for infected animals (Kluger et al., 1975). In this study,
395 *dipsosaurus dorsalis*, being poikilothermic animals, were moved from an environment
396 of 36 °C to 40 °C after bacterial infection, resulting in an increase in survival rates from
397 25% to 65% (Kluger et al., 1975). Similar results have since been observed in other
398 poikilotherms and some homeotherms. For instance, carp infected with Cyprinid
399 herpesvirus 3 (CyHV-3) move from lower temperatures of 24-28 °C to 32 °C, where

400 their survival rate reaches 100%, and viral load is significantly reduced (Rakus et al.,
401 2017). Behavioral fever responses to microbial infections have also been reported in
402 aquatic invertebrates such as freshwater crayfish (*Cambarus bartoni*), American lobster
403 (*Homarus americanus*), pink shrimp (*Penaeus duorarum*), horseshoe crab (*Limulus*
404 *polyphemus*), and *Penaeus vannamei* (Casterlin and Reynolds, 1978, 1979; M.E.
405 Casterlin, 1977; Rakhshaninejad et al., 2023). Despite these observations, the
406 antimicrobial immune mechanisms induced by febrile temperatures remain unclear.
407 The prevailing view that febrile temperatures benefit the host primarily suggests that
408 febrile response enhances innate and adaptive immune mechanisms in homeotherms
409 (Hasday et al., 2014). Our findings in the present study further support the enhancement
410 of innate immune mechanisms by febrile temperature in ectotherms such as shrimp and
411 *Drosophila* S2 cells. Additionally, elevated temperatures can cause some pathogenic
412 microorganisms to lose their optimal growth conditions. However, some
413 microorganisms have evolved strategies to exploit fever to enhance their invasion and
414 proliferation (Freitas Lione et al., 2010; Loh et al., 2013). Paradoxically, this further
415 underscores the benefits of fever for the host, as effective immune strategies exert
416 evolutionary pressure on pathogens, driving them to evolve counterstrategies to hijack
417 or block the febrile response.

418 HSFs are a type of evolutionarily conserved transcription factors initially known
419 for regulating the heat shock response (Anckar and Sistonen, 2011). However,
420 accumulating evidence indicates multiple additional functions beyond the activation of
421 HSPs, including roles in metabolism, immunity, disease, organismal aging and
422 longevity (Barna et al., 2018; Lee and Lee, 2022). Additionally, studies also reveal the
423 role of HSF1 in hormonal responses, which are evolved to maintain cellular
424 homeostasis and ensure the survival of organisms under changing environmental
425 conditions (Kumsta et al., 2017; Lee and Lee, 2022). HSF1 acts through a regulated
426 upstream promoter element called the heat shock element (HSE). HSEs are highly
427 conserved, including the inverted repeats of the pentameric sequence nGAAn (Amin et
428 al., 1988). The type of HSEs found in the proximal promoter regions of HSP genes
429 comprises at least three contiguous inverted repeats consisting of

430 nTTCnnGAAnnTTCn (Xiao and Lis, 1988). The discovery of novel HSF1 target genes
431 not involved in the heat shock response suggests that HSEs may be present in multiple
432 genes beyond HSPs (Barna et al., 2018). For instance, HSF1 can bind to the promoters
433 of CUP1, BTN2, SIS1, SGT2, and SSA3 genes, upregulating their transcriptional
434 activity to regulate oxidative stress (Morano et al., 2012). HSF1 also regulates the
435 hypothalamic-specific expression of the heat-inducible ion channel gene TRPV1,
436 suggesting a protective effect during fever (Fan-xin et al., 2012). In the present study,
437 we showed that a newly identified antimicrobial peptide, SWD, is specifically regulated
438 by LvHSF1 via two HSE motifs with the typical nGAAn sequence. Additionally, the
439 promoters of DmAMPs, such as Atta, CecA, and Def, also contain several HSE motifs
440 and are regulated by DmHSF1. Previous studies showed that the upstream sequence of
441 CrustinPm5 contains a putative promoter with an HSE motif, and the expression of
442 CrustinPm5 is upregulated upon heat treatment (Vatanavicharn et al., 2009). However,
443 there is currently no evidence that HSF1 directly binds to the HSE motif of AMPs in
444 invertebrates. Notably, our work is the first to show that HSF1 directly binds to the HSE
445 motifs of AMPs in shrimp and *Drosophila* S2 cells, suggesting this may be a conserved
446 regulatory mechanism in arthropods.

447 Although febrile temperature is generally believed to enhance host immunity, the
448 role of heat shock factors (HSFs) in viral infections is complex and varies across
449 different species and types of viral infections (Reyes et al., 2022). In vertebrates, HSF1
450 has been reported to participate in the transcription of HIV genes and their reactivation
451 from latency (Pan et al., 2016). Additionally, after orthopoxvirus infection, HSF1 is
452 phosphorylated, translocated into the nucleus, and increases the transcription of HSF1
453 target genes, benefiting the virus by extending the viral genome (Filone et al., 2014).
454 Conversely, stress-independent activation of HSF1 can reduce the quantity and
455 infectivity of HIV copies in a lymphoblastic cell line (Nekongo et al., 2020). Another
456 study reported that HSF1 could enable apoptosis-stimulating protein to reduce
457 autophagy in hepatocytes and inhibit HBV replication (Wang et al., 2021). In
458 invertebrates, DmHSF1-deficient adult flies are hypersensitive to DCV infection,
459 although the underlying mechanism has not yet been uncovered (Merkling et al., 2015).

460 HSF1 is also required for tolerance against several pathogenic agents in *Caenorhabditis*
461 *elegans* (Singh and Aballay, 2006). Similarly, the present study showed that HSF1 plays
462 a crucial role in antiviral immunity against WSSV infection, with knockdown of HSF1
463 *in vivo* leading to higher virus copies at low temperature (25 °C) and high temperature
464 (32 °C), and increased susceptibility to WSSV infection at high temperature (32 °C).
465 Notably, a recent study showed that ammonia stress-induced MjHSF1 upregulates the
466 expression of negative regulators that inhibit the production and function of interferon
467 analogs, enhancing WSSV infection in shrimp *Marsupenaeus japonicus* (Wang et al.,
468 2024). This may be because ammonia stress suppresses host immunity and increases
469 sensitivity to pathogenic infection in aquaculture (Weihrauch et al., 2018). In fact,
470 previous studies have shown that the optimal water temperature for *M. japonicus*
471 growth ranges from 25 to 32 °C, and a high temperature of 31 °C can reduce mortality
472 of WSSV-infected *M. japonicus* without increasing host immune response activity (You
473 et al., 2010). In contrast, the tolerance temperature for *L. vannamei* growth ranges from
474 7.5 to 42 °C, and our findings showed that elevated temperature can effectively enhance
475 the host's response to WSSV infection (Millard et al., 2021). Evidence also supports the
476 involvement of heat shock proteins in WSSV tolerance at elevated temperatures, with
477 heat shock protein 70 (HSP70) playing a crucial role in inhibiting WSSV replication at
478 high temperatures (32 °C) (Lin et al., 2011; Sun et al., 2014). These findings suggest
479 that the mechanism of elevated temperature protection against WSSV infection differs
480 between *M. japonicus* and *L. vannamei*. Therefore, our findings, together with those of
481 other studies, suggest that the benefit of HSF1 can be attributed to either the host or the
482 pathogen, depending on the nature and context of the host-virus-environment
483 interaction.

484 Antimicrobial peptides (AMPs) are pivotal components of innate immunity in
485 invertebrates, serving as the first line of defense against invading pathogens, including
486 bacteria, fungi, and viruses (Brogden, 2005). Typically, the transcription of AMPs is
487 regulated by the classical NF-κB and JAK/STAT pathways in invertebrates (Carpenter
488 and O'Neill, 2024). However, our results revealed that AMPs can also be regulated by
489 an alternative pathway mediated by HSF1 in shrimp and *Drosophila* S2 cells. In

490 crustaceans, various AMP families, including penaeidins, anti-lipopolysaccharide
491 factors, crustins, and stylicins, have been identified (Matos and Rosa, 2022). Among
492 these, the newly identified SWD belongs to type III crustins, characterized by a single
493 WAP domain (SWD) and a short N-terminal region. The most probable anti-WSSV
494 mechanism of SWD is its direct interaction with WSSV envelope proteins VP24 and
495 VP26, potentially inhibiting viral entry into target cells. VP24 has been identified as a
496 WSSV receptor-binding protein, interacting with the cellular receptor pIgR to mediate
497 WSSV entry into host cells (Niu et al., 2019). VP26 has been reported to bind to
498 SNAP29, inhibiting SNARE complex assembly and autophagic degradation (Liu et al.,
499 2024). Additionally, WSSV VP24, VP26, and VP28 form a complex termed an
500 "infectosome", which is crucial for WSSV infectivity (Li et al., 2015). Therefore, the
501 binding of SWD to WSSV envelope proteins VP24 and VP26 could disrupt WSSV
502 integrity and attenuate viral entry into shrimp cells.

503 In conclusion, our study demonstrates a conserved antiviral febrile response,
504 where the elevated temperature-induced HSF1-AMP axis plays a crucial role in
505 enhancing host resistance to viruses in shrimp and *Drosophila* S2 cells (Fig. 9).
506 Specifically, febrile temperature-induced HSF1 induces the expression of AMPs, which
507 directly bind to WSSV envelope proteins and block viral entry. Additionally, high
508 temperature restricts DCV replication in the invertebrate model system *Drosophila* S2
509 cells, also mediated by the HSF1-AMPs cascade. These findings highlight previously
510 unforeseen roles of HSF1 beyond the traditional heat shock response, revealing its
511 involvement in thermal regulation of immunity and the innate immune system's
512 response to thermal stress. Moreover, this study provides new avenues for managing
513 viral infections in arthropods, such as implementing varied pond depths for temperature
514 stratification as a cost-effective disease prevention method.

515

516

517

518 **4. Materials and methods**

519 ***Animal and pathogens***

520 Healthy specimens of *L. vannamei*, averaging 5 g each, were utilized for our
521 experiments. These specific pathogen-free (SPF) shrimp were sourced from Hisenor
522 Company's shrimp farm in Maoming, Guangdong Province, China. The shrimp were
523 maintained in a recirculating water tank system filled with air-pumped seawater at a
524 salinity of 25‰ and a constant temperature of 25 ℃. They were fed thrice daily to
525 satiation with a commercial shrimp diet provided by HAID Group, Guangzhou, China.
526 The inoculum for the WSSV, Chinese strain (AF332093), was prepared following
527 previously described methodologies (Li et al., 2018).

528 WSSV was extracted from the muscle tissue of WSSV-infected shrimp and
529 subsequently stored at –80 ℃. Prior to injection, the muscle tissue was homogenized
530 to prepare the WSSV inoculum, containing approximately 1 × 10^5 copies in 50 μl of
531 Phosphate-Buffered Saline (PBS; 140 mM NaCl, 2.7 mM KCl, 10 mM Na_2HPO_4, 1.8
532 mM KH_2PO_4, pH 7.4). For the pathogenic challenge experiments, each shrimp was
533 administered an intraperitoneal injection of 50 μl of the WSSV solution into the second
534 abdominal segment. Injections were performed using a 1-ml syringe (Becton Dickinson,
535 Shanghai, China).

536 Drosophila C Virus (DCV) were kindly provided by Professor Jiahuai Han's Lab.
537 The DCV was amplified in the S2 cells, after 3 days of infection, culture medium was
538 collected and centrifuged at 4 ℃ for 20 min (2,000 × *g*), then the supernatant was
539 collected and aliquots were frozen at –80 ℃.

540

541 ***Cells and cells assays***

542 *Drosophila* S2 cells (ATCC CRL 1963) were cultured at 28 °C in Schneider's Insect
543 Medium (Sigma-Aldrich, St. Louis, MO, USA) containing 10% fetal bovine serum
544 (Gibco, Grand Island, NY).

545 To knockdown *DmHSF1 in vitro*, 8 ×10^6 S2 were transfected with 15 μg dsRNA
546 in a 6-well plate by using FuGENE® HD Transfection Reagent (Promega Shanghai,
547 China), and transfected cells were incubated at 27 ℃ for 3 days before the transfection

548 and DCV infection assays according to a previously published method (Yang et al.,
549 2018).

550 For temperature assays, S2 cells were seeded into 6-well plate and then incubated
551 at 27 ℃ or 30 ℃ for 24 h, the transcription of DCV and DmHSF1 were detected by
552 qPCR. Besides, the same numbers of dsRNA-treated cells were infected with DCV at
553 a multiplicity of infection (MOI) of 10 in a 6-well plate at 27 ℃ or 30 ℃ for 24 h and
554 replaced with fresh medium, and the total RNA of S2 cells were extracted for qPCR
555 analysis.

556

557 ***Transcriptomic analysis***

558 Two groups of *L. vannamei* shrimp, Group W and Group TW, each comprising 30
559 individuals, were initially cultured at 25 ℃. For Group W, the shrimp were injected
560 with WSSV and continuously maintained at 25 ℃. In contrast, Group TW shrimp were
561 also injected with WSSV, but the culture temperature was raised to 32 ℃ within 3 hours
562 at 24 hours post-injection (hpi). At 12 hours post-temperature raising (hptr), gill
563 samples from 8 shrimp in both Group W and Group TW were collected. These samples
564 were immediately preserved in liquid nitrogen for subsequent analysis. Transcriptomic
565 sequencing was performed by LianChuan Biotech (Hangzhou, China). The FPKM
566 value was used to represent gene expression levels in each sample. The differential
567 expression between the two groups, each with three biological replicates, was
568 determined using DESeq2 software, accepting criteria of log2 (Fold Change) ≥ 1 and
569 an adjusted p-value ≤ 0.05. Gene annotations were provided for the *L. vannamei* shrimp
570 genome (Zhang et al., 2019). OmicShare tools (www.omicshare.com/tools) was used
571 to predict potential transcription factors and generate a heatmap.

572 To identify the genes whose expression was regulated by *LvHSF1*, healthy shrimp
573 were administered an intramuscular injection of 10 μg dsRNA targeting the *LvHSF1*
574 gene or *GFP* as a control. After 48 hours, shrimp were injected with 1×10^5 copies of
575 WSSV. At 24 hours post WSSV challenge, gill samples from 8 shrimp in both *dsHSF1*
576 and *dsGFP* were collected. These samples were immediately preserved in liquid
577 nitrogen for subsequent analysis. The sequencing and heatmap were performed

578 similarly to the above procedure.

579

580 ***RNA extraction, cDNA synthesis, and DNA and protein extraction***

581 Total RNA was extracted from different tissues of shrimp using the Eastep Super
582 Total RNA Extraction Kit (Promega, Shanghai, China). The genomic DNA of shrimp
583 tissues was extracted using a genomic DNA extraction kit (Vazyme, Nanjing, China).
584 First-strand cDNA synthesis was performed using a cDNA synthesis kit (Accurate
585 Biology, Hunan, China), according to the manufacturer's instructions. Protein samples
586 from gills and hemocytes were homogenized separately in IP lysis buffer (25 mM Tris-
587 HCl pH 7.4, 150 mM NaCl, 1 mM EDTA, 1% NP-40, 5% glycerin; Thermo Scientific,
588 Shanghai, China) with a protease and phosphatase inhibitor cocktail (Merck,
589 Kenilworth, NJ, USA), and then centrifuged at 12,000 × *g* for 10 minutes at 4 °C to
590 collect the supernatant for further analysis.

591

592 ***Tissue expression and immune challenge analysis by quantitative real-time PCR***
593 ***(qPCR)***

594 QPCR assays were performed to assess the mRNA levels in tissues expression
595 distribution, immune stimulation or the *in vivo* RNAi experiments. Expression levels
596 of *HSF1* (GenBank accession No. AHI13794), *SWD* (GenBank accession No.
597 PP786678) and *VP28* (GenBank accession No. NP_477943.1) were detected using
598 LightCycler480 System (Roche, Basel, Germany) in a final reaction volume of 10 μl,
599 which was comprised of 1 μl of 1: 10 cDNA diluted with ddH_2O, 5 μl of SYBR Green
600 Pro Taq HS Mix (Accurate Biology, Hunan, China) and 250 nM of specific primers
601 (Supplementary table 1).

602 For tissue distribution, shrimp were cultured at low temperature (25 °C) and high
603 temperature (32 °C). Shrimp tissues of epithelium, hemocyte, stomach, nerves, eyestalk,
604 gill, antenna, hepatopancreases, muscle, heart, intestine and pleopod were sampled and
605 pooled from 15 shrimp. For immune stimulation, the treated group were injected with
606 5 μg polyinosinic-polycytidylic acid (Poly (I: C)) or 50 μl WSSV (~1×10^5 copies), and
607 the control group was injected with PBS solution. Hemocyte, gill and intestine of

608 challenged shrimps were collected at 0, 4, 8, 12, 24, 36, 48, and 72 h after injection.
609 The cycling program were performed as described previously (Xiao et al., 2021). The
610 expression of each gene was calculated using the Livak ($2^{-\Delta\Delta CT}$) method after
611 normalization to *EF-1α* (GenBank accession No. GU136229) and *β-Actin* (GenBank
612 accession No. AF186250). Primer sequences are listed in Supplementary table 1.
613 The transcription of *DCV*, *DmHSF1* (GenBank accession No. NM_057227.5) and
614 *DmAMPs* were also detect by quantitative real-time PCR. The expression of each gene
615 was calculated using the Livak ($2^{-\Delta\Delta CT}$) method after normalization to *DmRpL32*
616 (GenBank accession No. NP_733340.1). Primer sequences are listed in Supplementary
617 table 1.
618
619 ***Detection of viral loads by absolute quantitative PCR***
620 To measure viral titers in shrimp, absolute quantitative PCR (ab-qPCR) was
621 employed. This process utilized a set of primers, wsv069 (WSSV32678-
622 F/WSSV32753-R), targeting a single-copy gene of the WSSV, along with a Taq-Man
623 fluorogenic probe (WSSV32706), as detailed in previous studies. Gill tissue samples
624 were collected from WSSV-infected shrimp. DNA extraction from these samples was
625 conducted using previously described methods (Fu et al., 2022). The concentration of
626 WSSV genome copies was quantified by ab-qPCR, using the specific primers
627 WSSV32678-F/WSSV32753-R and the TaqMan fluorogenic probe, as listed in
628 Supplementary table 1. To ensure accuracy, each shrimp sample underwent three
629 replicates of ab-qPCR. The number of WSSV genome copies was calculated and
630 normalized against 0.1 μg of shrimp tissue DNA.
631
632 ***Recombinant protein expression and purification***
633 The coding sequences of SWD (without the signal peptide, 1-26 amino acids) was
634 amplified by PCR using corresponding primers (Supplementary table 1) and subcloned
635 into pET-32a (+) plasmid (Merck Millipore, Darmstadt, Germany). After confirmed by
636 sequencing, the recombinant plasmid was transferred into *E. coli* Rosetta (DE3) cells
637 (TransGen Biotech, Beijing, China). Then, positive clones harboring the desired

638 fragment were selected for inducing expression. After 4 hours of induction with 0.1
639 mM Isopropyl β-D-Thiogalactoside (IPTG) at 30 ℃, cells were pelleted by
640 centrifugation and sonicated for 30 minutes on ice water. The supernatant from the
641 sonicated proteins was purified by using Ni-NTA agarose (Qiagen, Düsseldorf,
642 Germany) according to the manufacturer's instructions. The rTrx-His-tag, GST and
643 HSF1-GST proteins were induced and purified in the same way. The purified proteins
644 were checked by Coomassie staining or Western blot analysis. The concentration of the
645 purified proteins was determined using a BCA protein assay kit (Beyotime
646 Biotechnology, Shanghai, China).
647
648 ***SDS-PAGE and western blotting***
649 Western blotting was performed to evaluate the protein levels of LvHSF1, VP28,
650 DCV, the purified SWD, rTrx-His-tag and LvHSF1-GST. And then the proteins were
651 separated on 12.5% SDS-PAGE gels and then transferred to polyvinylidene difluoride
652 (PVDF) membranes (Merck Millipore, Darmstadt, Germany). After blocking with 5%
653 nonfat milk diluted in Tris Buffered Saline with Tween 20 (TBST) buffer (150 mM
654 NaCl, 0.1% Tween-20, 50 mM Tris-HCl, pH 8.0) for 1 hour, and the membrane was
655 incubated with 1: 1000 polyclonal rabbit anti-LvHSF1 (produced in Gene Create,
656 Wuhan, China), 1: 1000 polyclonal rabbit anti-VP28 (produced in Abmart, Shanghai,
657 China), 1: 1000 polyclonal rabbit anti-DCV capsid polyprotein (Abcam, Cambridge,
658 UK), 1:1000 mouse anti-6 × His (Sigma, St Louis, MO, USA) or 1:1000 mouse anti-
659 GST (TransGen Biotech, Beijing, China) for 2 hours at 25 °C. The PVDF membranes
660 were washed for three times with TBST and then incubated with 1:5000 goat anti-rabbit
661 IgG (H+ L) HRP or 1:5000 goat anti-mouse IgG (H+ L) HRP secondary antibody
662 (Promega, Shanghai, China) for 1 hour. Membranes were developed using an enhanced
663 chemiluminescent blotting substrate (Thermo Fisher Scientific, Waltham, MA, USA),
664 and the chemiluminescent signal was detected using the 5200 Chemiluminescence
665 Imaging System (Thermo Fisher Scientific, Waltham, MA, USA).
666
667 ***Knockdown of specific genes by RNA interference (RNAi)***

668 The T7 RiboMAX Express RNAi System kit (Promega, Shanghai, China) was
669 employed for the synthesis of double-stranded RNA (dsRNA) targeting *HSF1*, *SWD*
670 and *GFP*. The specific primers used for dsRNA synthesis are listed in Supplementary
671 table 1. The integrity and quality of the synthesized dsRNA were verified using 1.5%
672 agarose gel electrophoresis and quantified with a NanoDrop 2000 spectrophotometer
673 (Thermo Scientific, Shanghai, China). For the experimental treatments, shrimp were
674 injected with 2 μg/g of body weight of the respective dsRNAs, dissolved in 50 μl of
675 PBS. Control groups received injections of GFP dsRNA and PBS. Hemocytes and gills
676 were collected from the shrimp 48 hours post-dsRNA injection. Total RNA was
677 extracted from the collected tissue samples. The efficiency of RNAi was evaluated by
678 qPCR using the corresponding primers for each gene. This assessment aimed to confirm
679 the knockdown of the targeted genes in the experimental groups compared to the
680 controls as described previously (Li et al., 2024).
681
682 ***Survival assays***
683 Healthy shrimp were divided into two groups (n = 30 each) and received an
684 intramuscular injection of 10 μg dsRNA solution (HSF1 dsRNA or GFP dsRNA diluted
685 in PBS). After 48 hours post dsRNA injection, the shrimp in each group were injected
686 again with 1×10^5 copies of WSSV particles diluted in 50 μl PBS. The first group was
687 maintained at low temperature (25 °C), the second at a high temperature (32 °C). The
688 survival rates of each group were recorded at 4-hour intervals.
689 To knockdown the expression of SWD, healthy shrimp were administered an
690 intramuscular injection of 10 μg dsRNA targeting the *SWD* gene or PBS as a control.
691 After 48 hours, shrimp were injected with 1×10^5 copies of WSSV, with a parallel group
692 receiving a mock challenge with PBS (n = 30). To evaluate the effect of recombinant
693 rSWD on WSSV replication *in vivo*, rescue experiments were conducted. Shrimp (n =
694 30) were co-injected with 10 μg rSWD or rTRX along with the WSSV inoculum. The
695 survival rates of each group were recorded at 4-hour intervals. Differences in survival
696 between groups were analyzed using the Mantel-Cox (log-rank χ^2 test) method,
697 employing GraphPad Prism software (GraphPad Software, La Jolla, CA, USA).

698

699 ***Dual-luciferase reporter assays***

700 The partial promoter sequence with 2000 bp upstream of SWD was cloned using
701 the specific primers (Supplementary table 1) and then linked into pGL3-Basic (Promega,
702 Shanghai, China) to generate pGL3-SWD (reporter plasmid). The vector pGL3-SWD-
703 M1, pGL3-SWD-M2 and pGL3-SWD-M1/2 with mutant of the HSF1 binding motif
704 were also generated, respectively. *Drosophila* S2 cell was used instead in order to detect
705 the effects of HSF1 on the promoters of SWD. For dual-luciferase reporter assays, S2
706 cells were plated into a 96-well plate, and 12 hours later, the cells of each well were
707 transfected with 0.05 μg of firefly luciferase reporter gene plasmids, 0.001 μg pRL-TK
708 renilla luciferase plasmid (Promega Shanghai, China), or 0.05 μg proteins expression
709 plasmids or empty pAc5.1A plasmids (as controls) using the Fugene HD Transfection
710 Reagent (Promega Shanghai, China) according to the user manual. Forty-eight hours
711 post-transfection, the dual-luciferase reporter assays were performed in order to
712 calculate the relative ratios of firefly and renilla luciferase activities using the Dual-Glo
713 Luciferase Assay System kit (Promega Shanghai, China), according to the
714 manufacturer's instructions. All experiments were repeated six times.

715 To explore the regulatory activity of DmHSF1 on the DmAMPs (Atta, CecA and
716 Def), we constructed the vector pGL3-Atta, pGL3-CecA and pGL3-Def. And the vector
717 pGL3-Atta, pGL3-CecA and pGL3- Def with mutant of the HSF1 binding motif were
718 also generated, respectively. The dual-luciferase reporter assays were conducted in the
719 same way.

720

721 ***EMSA assay***

722 EMSA was performed using a Light Shift Chemiluminescent EMSA kit (Thermo
723 Fisher Scientific, Waltham, MA, USA) according to a previously published method
724 (Wang et al., 2020). Briefly, the biotin-labeled or unbiotin-labeled probes were designed
725 using the *HSF1* binding motif sequence (5'- CTATAGAACCATC-3' and 5'-
726 GACTTTTCGAGGA -3'). The mutant probe was designed via mutating the HSF1
727 binding motif sequence. All of the probes were synthesized by Ruibo Technologies

728 (Guangzhou, China), and sequences are listed in Supplementary table 1. In brief, the
729 recombinant proteins (10 μg) of HSF1 were incubated with 20 fmol of the probes for
730 the binding reactions. The reactions were separated on a 5% native PAGE gel,
731 transferred to positively charged nylon membranes (Roche, Germany), and cross-linked
732 by UV light. Then the biotin-labeled DNA on the membrane was detected by
733 chemiluminescence and developed on x-ray film, followed by enhanced
734 chemiluminescence (ECL) visualization (Tanon, Shanghai, China).
735
736 ***Pull-down assays***
737 Pull-down assays were performed to explore whether the recombinant rSWD
738 could interact with the main envelope proteins of WSSV (VP19, VP24, VP26 and
739 VP28). The recombinant GST-tagged VP19, VP24, VP26 and VP28 were obtained from
740 our previous studies (Xiao et al., 2020). For GST pull-down assays, 5 μg rSWD was
741 incubated with 5 μg of GST-tagged WSSV protein solution at 4 ℃ for 3 h by agitation.
742 Subsequently, 20 μl of the GST resin were added and the agitation continued for another
743 2 h. The resin was washed four times with PBS. Finally, the resins were re-suspended
744 in 50 μl of the SDS-PAGE sample buffer, boiled and analyzed by Western blot analysis
745 using 6 × His antibody. For His pull-down assays, 5 μg rSWD was incubated with 5 μg
746 of GST-tagged WSSV protein solution at 4 ℃ for 3 h by agitation. Subsequently, 20 μl
747 of the Ni-NTA binding resin were added and the agitation continued for another 2 h.
748 The resin was washed four times with PBS. Finally, the resins were re-suspended in 50
749 μl of the SDS-PAGE sample buffer, boiled and analyzed by Western blot analysis using
750 GST-tag antibody.
751
752 ***Immunocytochemical staining***
753 Immunocytochemical staining was used to observe the co-localization of SWD
754 and WSSV VP proteins. *Drosophila* S2 cells were seeded onto poly-L-lysine-treated
755 glass cover slips in a 24-well plate with approximate 40% confluent. The S2 cells of
756 each well were transfected with 0.5 μg pAc5.1-SWD-Flag, pAc5.1-VP24-HA or
757 pAc5.1-VP26-HA using the MIK-3000 Transfection Reagent (MIKX, Shenzhen,

China). Thirty-six hours post plasmid transfection, cell culture medium was removed, and cells washed with PBS three times. Cells were then fixed with 4% paraformaldehyde at 25 °C for 15 min following with methanol permeabilization at -20 °C for 10 min. After washing sides for three times, cells were blocked with 3% bovine serum albumin (dissolved in PBS) for 60 min at 25 °C and then incubated with rabbit anti-HA antibody (CST, 1:300 diluted in 2% BSA) and mouse anti-Flag antibody (CST, 1:300 diluted in 2% BSA). The slides were then washed with PBS three times and then incubated with anti-rabbit IgG (H+L) Alexa Fluor 488 (CST, 1:1000 diluted in 2% BSA) and anti-mouse IgG (H+L) Alexa Fluor 594 (CST, 1:1000 diluted in 2% BSA) for 60 min at 25 °C in the dark. The cell nuclei were stained with Hoechst (Beyotime, Shanghai, China; cat. no. C1002) for 5 min. Finally, fluorescence was visualized on a confocal laser scanning microscope (Leica TCS-SP8, Wetzlar, Germany).

Statistical analysis

All data were presented as means ± SD. Student's *t* test was used to calculate the comparisons between groups of numerical data. For survival rates, data were subjected to statistical analysis using GraphPad Prism software (Graphpad, San Diego, CA, USA) to generate the Kaplan–Meier plot (log-rank χ^2 test).

Declaration of interest statement: All authors declare that the research was conducted in the absence of any commercial or financial relationships that could be construed as a potential conflict of interest.

Author contributions: Chaozheng Li, Jianguo He and Bang Xiao conceived and designed the experiments. Bang Xiao, Shihan Chen, Yue Wang, Xuzheng Liao and Chaozheng Li performed the experiments and analyzed data. Bang Xiao, Shihan Chen, Yue Wang, Xuzheng Liao and Chaozheng Li wrote the draft manuscript. Chaozheng Li and Jianguo He acquired finding. Chaozheng Li was responsible for forming the hypothesis, project development, data coordination, and writing, finalizing, and submitting the manuscript. All authors discussed the results and approved the final version.

Acknowledgement: This research was supported by National Key Research and Development Program of China (2022YFF1000304), National Natural Science Foundation of China (32022085/31930113/32373158), Southern Marine Science and Engineering Guangdong Laboratory (Zhuhai) (SML2023SP234), China Postdoctoral Science Foundation (2023M743987), and Guangdong Basic and Applied Basic Research Foundation (2023A1515110528). The funders had no role in study design, data collection and analysis, decision to publish, or preparation of the manuscript.

Data availability: All reagents and experimental data are available within transparent methods or from corresponding author upon reasonable request.

Ethics statement: All animal experiments were approved by Institutional Animal Care and Use Committee of Sun Yat-Sen University (Approval No. SYSU-IACUC-2023-B0005).

Figures and Figure legends

Figure 1.

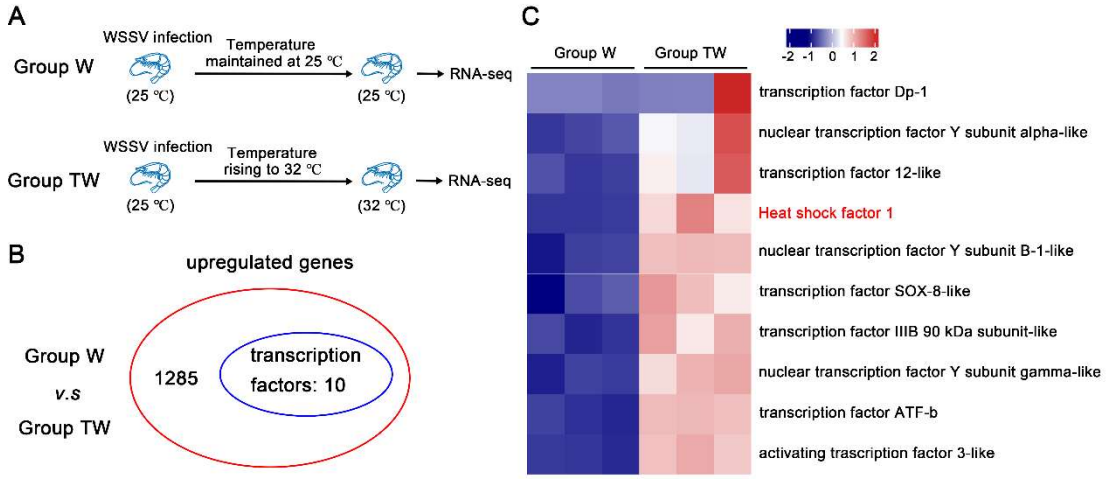

Figure 1. Identification of HSF1 as a key factor induced by high temperature.

(A) Diagram illustration of the experimental setup for transcriptome analysis. Group W was injected with WSSV and maintained continuously at 25 °C. In contrast, Group TW, also injected with WSSV, had their culture temperature increased to 32°C at 24 hours post-injection (hpi).

(B) Identification of high temperature-induced genes by RNA-Seq. RNA sequencing was performed 12 hours post-temperature increase. Gill samples from 8 shrimp in each group were collected for Illumina sequencing (NCBI SRA database accession number PRJNA1050424).

(C) Heatmap showing the differential expression of upregulated genes encoding potential transcription factors. The heatmap displays the fragments per kilobase per transcript per million mapped reads (FPKM) values from three biological replicates, shown after logarithmic transformation.

836 **Figure 2.**

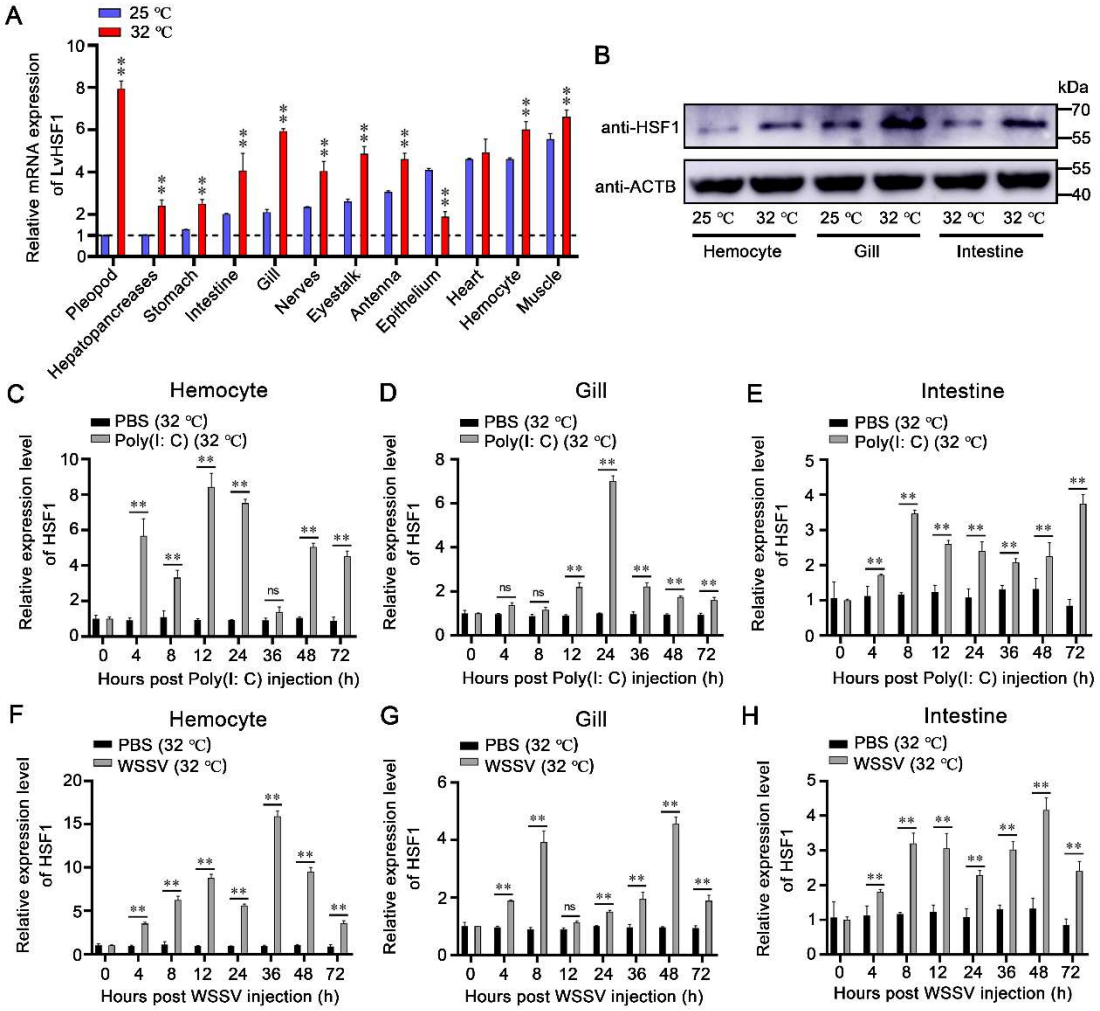

837

838 **Figure 2. Upregulation of LvHSF1 in shrimp challenged by WSSV at both low**
839 **(25 °C) and high (32 °C) temperatures.**

840 **(A)** Transcriptional expression of LvHSF1 in different tissues of healthy shrimp
841 subjected to low (25 °C) and high (32 °C) temperatures for 12 hours. The pleopod tissue
842 at 25 °C serves as a reference, with its expression level set to 1.0. Expression values
843 were normalized against EF-1α and β-Actin using the Livak ($2^{-\Delta\Delta CT}$) method. Data
844 represent the mean ± SD from triplicate assays.

845 **(B)** Protein levels of HSF1 at 25 °C and 32 °C detected by western blotting.

846 **(C-E)** Expression profiles of LvHSF1 after Poly (I:C) injection at high temperatures
847 (32 °C) in hemocytes (C), gills **(D)** and intestines (E). Expression levels were measured
848 by qPCR, normalized against EF-1α and β-Actin using the Livak ($2^{-\Delta\Delta CT}$) method, and
849 presented as mean ± SD from triplicate assays.

850 **(F-H)** Expression profiles of LvHSF1 after WSSV injection at high temperatures (32 °C)
851 in hemocytes (F), gills (G) and intestines (H). Expression levels were measured by
852 qPCR, normalized against EF-1α and β-Actin using the Livak ($2^{-\Delta\Delta CT}$) method, and
853 presented as mean ± SD from triplicate assays.
854 Statistical significance was calculated using the Student's *t*-test ($^{**}p < 0.01$, $^{*}p < 0.05$).
855 All experiments were representative of three biological replicates and yielded similar
856 results.
857

858 **Figure 3.**

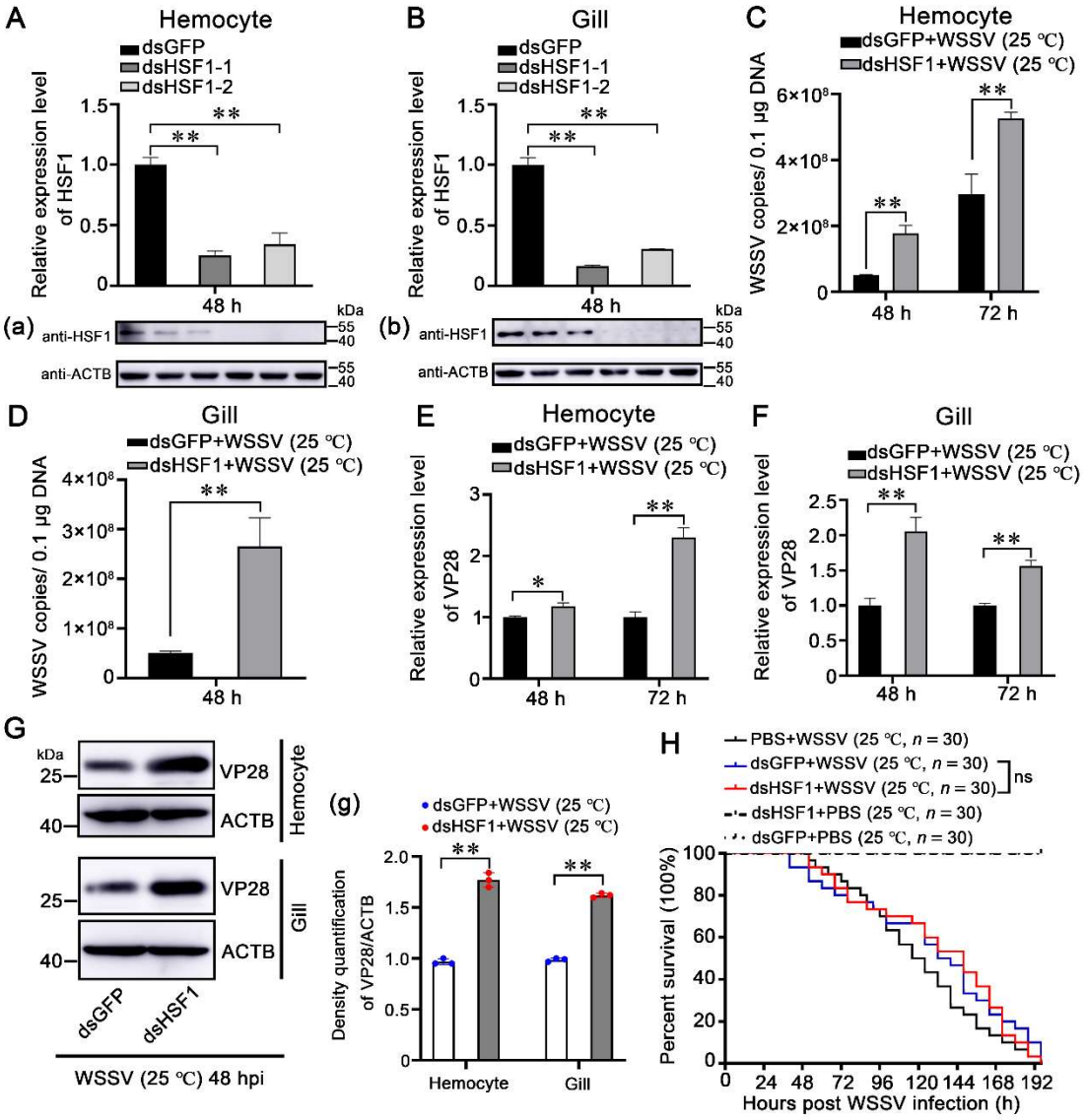

859

860 **Figure 3. Role of HSF1 in restricting WSSV replication in shrimp at low (25 °C)**
861 **temperatures.**

862 **(A, B)** Silencing Efficiency of dsRNA-LvHSF1. The efficacy of two dsRNA-LvHSF1
863 constructs (dsLvHSF1-1 and dsLvHSF1-2) was assessed by qPCR in hemocytes (A)
864 and gills (B). Additionally, protein levels of LvHSF1 were evaluated by western
865 blotting in both tissues (panels a and b). Expression values were normalized against EF-
866 1α and β-Actin using the Livak ($2^{-\Delta\Delta CT}$) method. Data represent the mean ± SD from
867 triplicate assays.

868 **(C, D)** Quantification of WSSV copies. The quantity of WSSV copies in hemocytes (C)
869 and gills (D) at low temperature (25 °C) post-WSSV infection was determined using

870 absolute quantitative PCR.

871 **(E, F)** Transcriptional expression of the VP28 gene. The transcriptional expression of
872 the VP28 gene was analyzed by qPCR in hemocytes (E) and gills (F) at low temperature
873 (25 °C) following WSSV infection.

874 **(G)** Expression of WSSV VP28 protein. Expression of WSSV VP28 protein was
875 detected by western blotting in hemocytes and gills at low temperature (25 °C) after
876 WSSV infection. Quantification and statistical analysis of three independent repeats
877 were performed using ImageJ (panel g).

878 **(H)** Survival rates of WSSV-infected shrimp post-LvHSF1 knockdown. The survival
879 rates of WSSV-infected shrimp post-LvHSF1 knockdown were monitored at low
880 temperature (25 °C), with recordings made every 4 hours.

881 Statistical analysis was performed using the Kaplan-Meier plot (log-rank χ^2 test). All
882 experiments were conducted with three biological replicates, consistently yielding
883 similar results.

884

885 **Figure 4.**

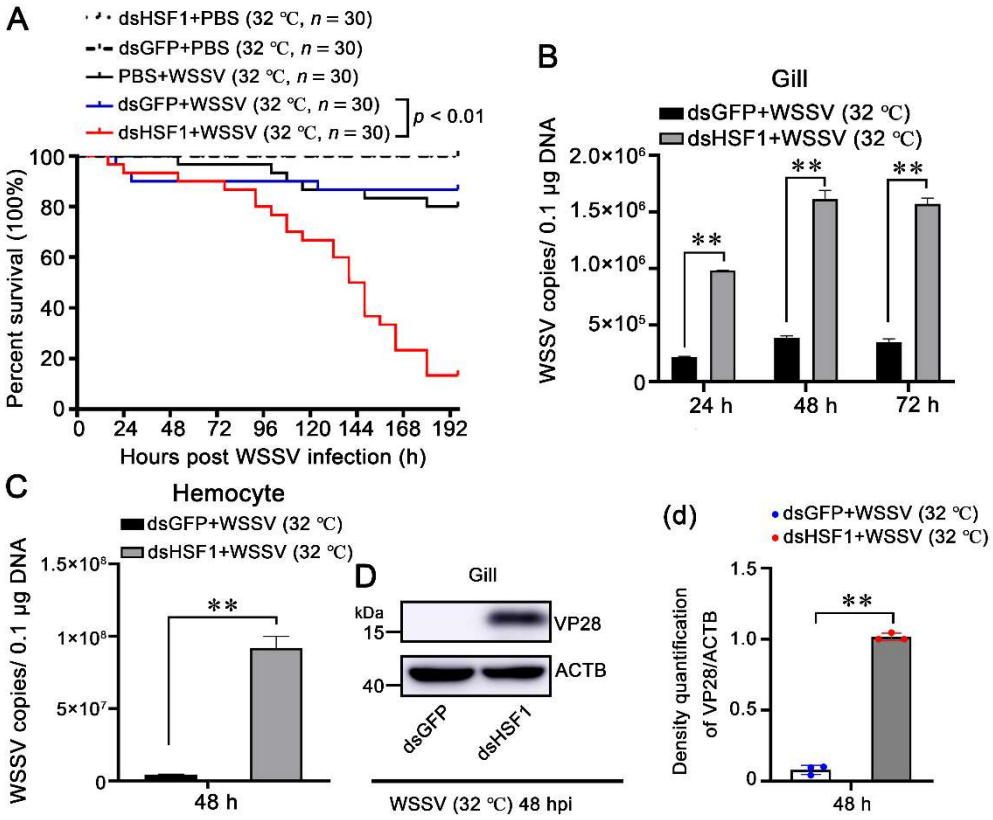

886

887 **Figure 4. Role of HSF1 in restricting WSSV replication in shrimp at high (32 ℃)**
888 **temperatures.**

889 **(A)** Survival rates of WSSV-infected shrimp post-LvHSF1 knockdown. The survival
890 rates of WSSV-infected shrimp post-LvHSF1 knockdown were monitored at high
891 temperature (32 °C), with recordings made every 4 hours. Statistical analysis was
892 performed using the Kaplan-Meier plot (log-rank χ^2 test).

893 **(B, C)** Quantification of WSSV copies. The quantity of WSSV copies in gills (B) and
894 hemocytes (C) at high temperature (32 °C) post-WSSV infection was determined using
895 absolute quantitative PCR.

896 **(D)** Expression of WSSV VP28 protein. Expression of WSSV VP28 protein was
897 detected by western blotting in gills at high temperature (32 °C) after WSSV infection.
898 Quantification and statistical analysis of three independent repeats were performed
899 using ImageJ (panel d). Statistical significance was calculated using the Student's *t*-test
900 (**$p < 0.01$). All experiments were conducted with three biological replicates,
901 consistently yielding similar results.

902 **Figure 5.**

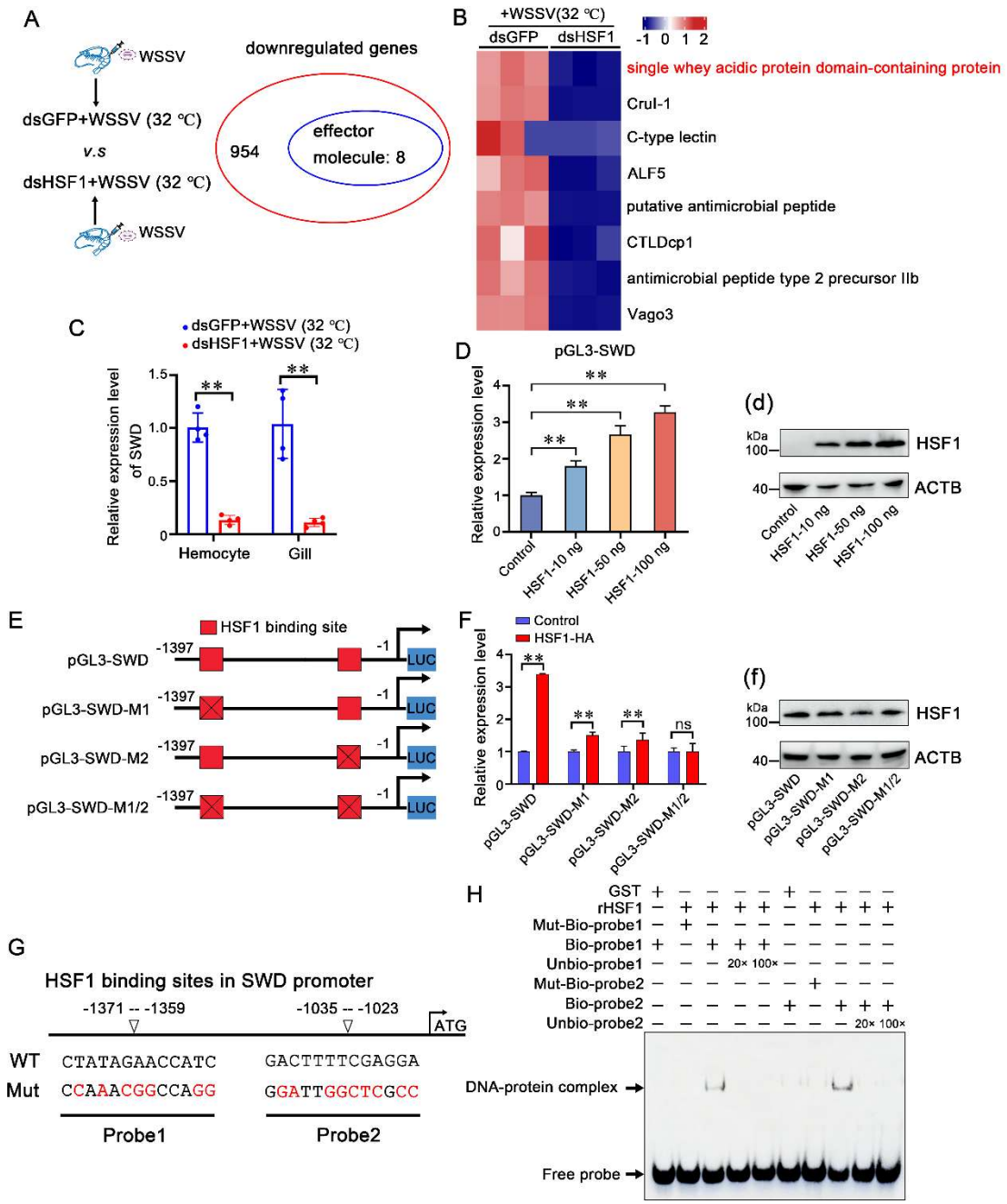

903

904 **Figure 5. SWD is a potential antiviral effector regulated by HSF1.**

905 **(A)** Venn diagram showing the downregulated genes by RNA-Seq. RNA-seq was
906 performed 24 hours after WSSV infection (NCBI SRA database accession number
907 PRJNA1110613).

908 **(B)** Heatmap showing the differential expression of downregulated genes encoding
909 potential effector molecules. The color bar indicates the gradient of normalized
910 expression levels.

(C) mRNA transcription levels of SWD in hemocytes and gills. mRNA transcription levels of SWD in the hemocytes and gills of LvHSF1-silenced shrimp under WSSV challenge.

(D) Dual-luciferase reporter assays. Dual-luciferase reporter assays were performed to analyze the effects of overexpression of LvHSF1 on the promoter activities of SWD in *Drosophila* S2 cells in a dose-dependent manner. Protein expression of LvHSF1 was detected with anti-HA Ab, with β-actin used as a protein loading control (panel d).

(E) Schematic diagram of the SWD promoter regions. Schematic diagram of the SWD promoter regions in the luciferase reporter gene constructs. The HSF1 binding motif sites are shown in red rectangles.

(F) Dual-luciferase reporter assays with mutated HSF1 binding motifs. Dual-luciferase reporter assays were performed to analyze the effects of overexpression of LvHSF1 on the promoter activities of SWD with mutated HSF1 binding motifs. Protein expression of LvHSF1 was detected with anti-HA Ab, with β-actin used as a protein loading control (panel f).

(G) Analysis of the SWD promoter. The HSF1 binding site was analyzed using the online JASPAR database.

(H) EMSA assay. LvHSF1 protein interaction with HSF1 binding sites from the SWD promoter was analyzed *in vitro* by EMSA assay. Competition assays were performed in the presence of excess unlabeled probes.

Statistical significance was calculated using the Student's *t*-test ($^{**}p < 0.01$, $^{*}p < 0.05$). All experiments were conducted with three biological replicates, consistently yielding similar results.

941 **Figure 6.**

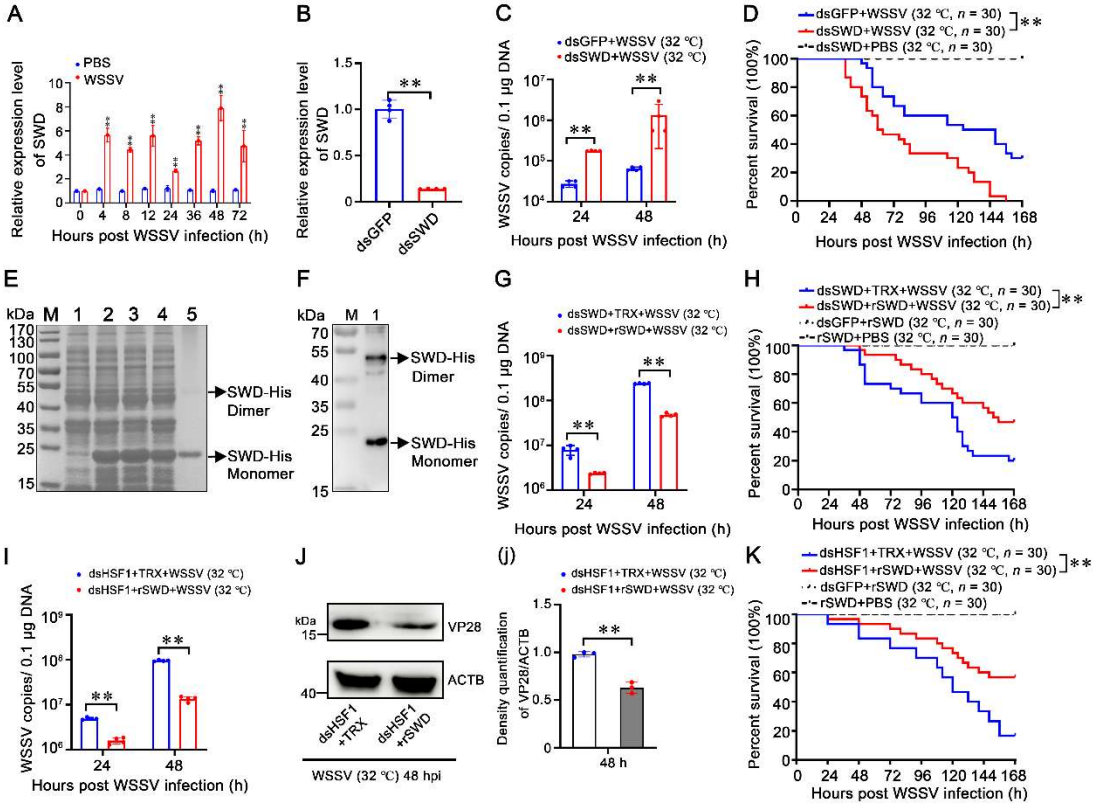

942

943 **Figure 6. *SWD* possessed potent antiviral activities against WSSV.**

944 **(A)** Expression of SWD in gills from WSSV-challenged shrimp.

945 **(B)** Silencing efficiency of SWD in gills. Silencing efficiency of SWD in gills 48 hours
946 after WSSV infection.

947 **(C)** Quantity of WSSV copies in gills at high temperature (32 °C). The quantity of
948 WSSV copies in gills at high temperature (32 °C) was detected by absolute quantitative
949 PCR at 24 and 48 hours after WSSV infection. DsGFP was used as a control.

950 **(D)** Survival rates of WSSV-infected shrimp post-SWD knockdown. Survival rates of
951 WSSV-infected shrimp post-SWD knockdown at high temperature (32 °C) were
952 monitored, with recordings made every 4 hours. Statistical analysis was performed
953 using the Kaplan-Meier plot (log-rank χ^2 test).

954 **(E)** SDS-PAGE analysis of recombinant SWD protein expressed in *E. coli*. Line 1:
955 Uninduced *E. coli* transformed with SWD; Line 2: Induced *E. coli* transformed with
956 SWD; Line 3: Supernatant of ultrasonic lysed *E. coli* expressing SWD; Line 4:
957 Precipitate of lysed *E. coli* expressing SWD. Line 5: Purified recombinant SWD protein

958 (black arrow).

959 **(F)** Western blotting of purified rSWD protein. Purified rSWD protein was checked by
960 Western blotting with anti-6×-His Ab.

961 **(G)** Quantity of WSSV copies in shrimp gills following SWD application post-SWD
962 knockdown. The quantity of WSSV copies in shrimp gills following 10 μg SWD
963 application post-SWD knockdown at high temperature (32 °C) was measured *in vivo* at
964 24 and 48 hours using absolute quantitative PCR.

965 **(H)** Survival rates post-rSWD application. Shrimp were injected with 10 μg rSWD or
966 control protein, mixed with WSSV inoculum post-SWD knockdown at high
967 temperature (32 °C). Survival rates were recorded every 4 hours.

968 **(I)** Quantity of WSSV copies in shrimp gills following SWD application post-LvHSF1
969 knockdown. The quantity of WSSV copies in shrimp gills following 10 μg SWD
970 application post-LvHSF1 knockdown at high temperature (32 °C) was measured *in vivo*
971 at 24 and 48 hours using absolute quantitative PCR.

972 **(J)** Expression of WSSV VP28 protein. Expression of WSSV VP28 protein was
973 detected by Western blotting in gills at high temperature (32 °C) after WSSV infection.
974 Quantification and statistical analysis of three independent repeats were performed
975 using ImageJ (panel j).

976 **(K)** Survival rates post-rSWD application. Shrimp were injected with 10 μg rSWD or
977 control protein, mixed with WSSV inoculum post-LvHSF1 knockdown at high
978 temperature (32 °C). Survival rates were recorded every 4 hours.

979 Statistical significance was calculated using the Student's *t*-test (**$p < 0.01$, *$p < 0.05$).
980 All experiments were conducted with three biological replicates, consistently yielding
981 similar results.

982

983 **Figure 7.**

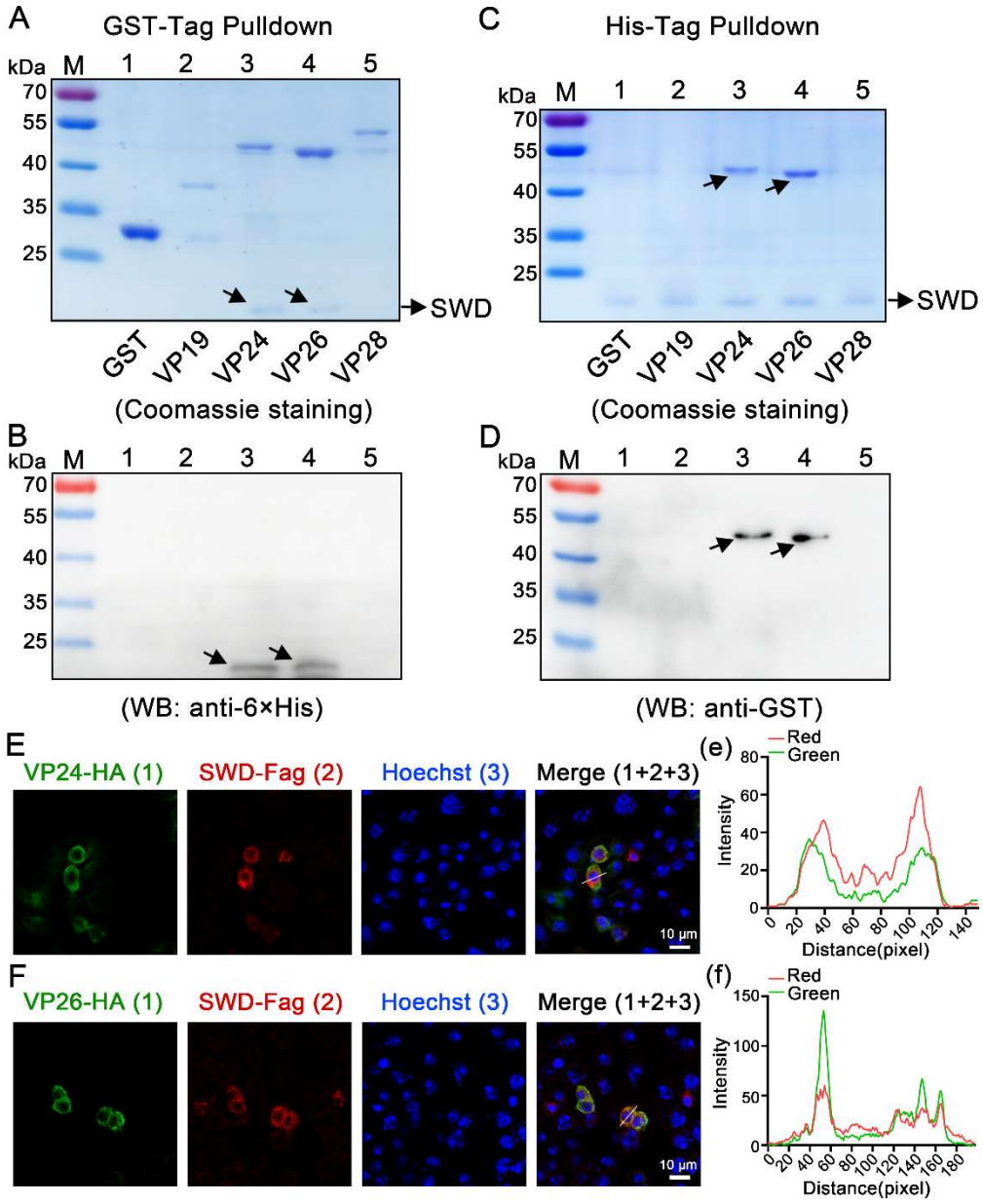

984

985 **Figure 7. SWD interacts with envelope proteins of WSSV.**

986 **(A, B)** GST pull-down assay for the detection of the interaction between rSWD with
987 VP19, VP24, VP26, and VP28. The results were shown via staining with Coomassie
988 blue (A) or Western blotting using 6×-His Ab (B). The GST-tag protein was used as a
989 control.

990 **(C, D)** His pull-down assay for the detection of the interaction of rSWD with VP19,
991 VP24, VP26, and VP28 via Coomassie blue staining (C) or Western blotting using the
992 GST-tag Ab (D). The GST tag protein was used as a control.

993 **(E, F)** The colocalization of SWD with VP24 and VP26 in S2 cells, 24 hours post-

994 plasmid transfection. VP24 and VP26 was detected with rabbit anti-HA antibodies and
995 anti-rabbit Alexa Fluor 488, while SWD was identified using anti-Flag antibodies and
996 anti-mouse Alexa Fluor 594. DAPI staining highlighted the nuclei. The scale bar
997 represents 10 μm. (e-f) Quantitative analysis of fluorescence colocalization.
998 Colocalization intensity was quantitatively analyzed, with complete colocalization
999 indicated by overlapping peaks and maxima shifted by less than 20 nm.
1000 All experiments were representative of three biological replicates and yielded similar
1001 results.
1002

1003 **Figure 8.**

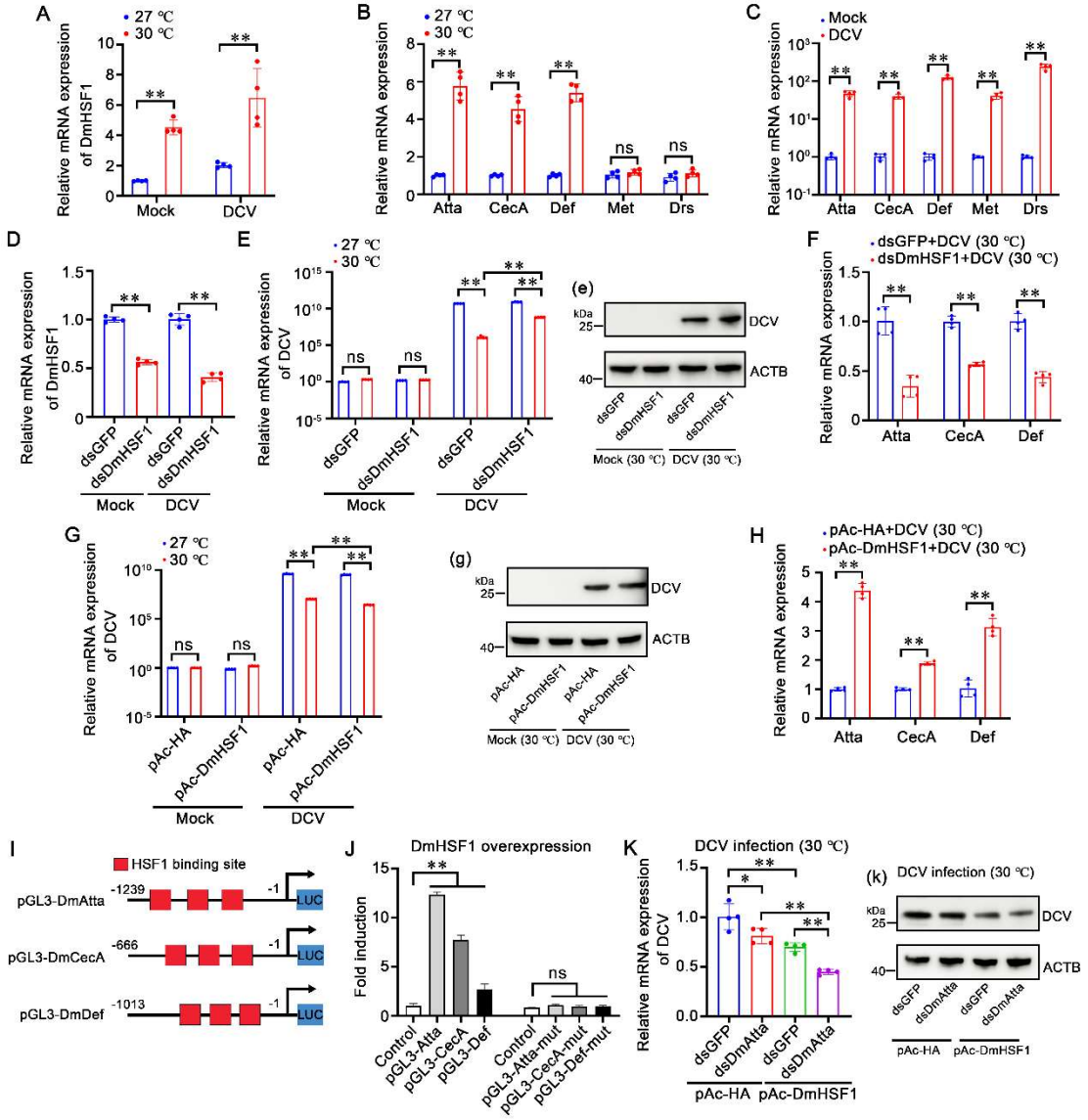

1004

1005 **Figure 8. High temperature-induced DmHSF1-AMPs axis restricts DCV**
1006 **replication in *Drosophila*** S2 cells**.**

1007 **(A)** Transcriptional expression of DmHSF1. Transcriptional expression of DmHSF1 in
1008 S2 cells with or without DCV infection at low (27 °C) and high (30 °C) temperatures.

1009 **(B)** Transcriptional expression of DmAMPs. Transcriptional expression of DmAMPs
1010 in S2 cells at low (27 °C) and high (30 °C) temperatures.

1011 **(C)** Transcriptional expression of DmAMPs with or without DCV infection.
1012 Transcriptional expression of DmAMPs in S2 cells with or without DCV infection.

1013 **(D)** Silencing efficiency of DmHSF1. Silencing efficiency of DmHSF1 in S2 cells 24
1014 hours after dsRNA application with or without DCV infection.

1015 **(E)** mRNA expression of DCV. mRNA expression of DCV at low (27 °C) and high
1016 (30 °C) temperatures after DmHSF1 knockdown, with dsGFP used as a control. (e)
1017 Protein expression of DCV at low (27 °C) and high (30 °C) temperatures after DmHSF1
1018 knockdown.
1019 **(F)** mRNA expression of DmAMPs. mRNA expression of DmAMPs at low (27 °C) and
1020 high (30 °C) temperatures after DmHSF1 knockdown and DCV infection.
1021 **(G)** mRNA expression of DCV after DmHSF1 overexpression. mRNA expression of
1022 DCV at low (27 °C) and high (30 °C) temperatures after DmHSF1 overexpression. (g)
1023 Protein expression of DCV at low (27 °C) and high (30 °C) temperatures after DmHSF1
1024 overexpression.
1025 **(H)** mRNA expression of DmAMPs after DmHSF1 overexpression. mRNA expression
1026 of DmAMPs at low (27 °C) and high (30 °C) temperatures after DmHSF1
1027 overexpression and DCV infection.
1028 **(I)** Schematic Diagram of DmAMPs Promoter Regions. Schematic diagram of the
1029 DmAMPs promoter regions in the luciferase reporter gene constructs. The HSF1
1030 binding motif sites are shown in red rectangles.
1031 **(J)** Dual-luciferase reporter assays. Dual-luciferase reporter assays were performed to
1032 analyze the effects of DmHSF1 overexpression on the promoter activities of DmAMPs
1033 with or without mutated HSF1 binding motifs.
1034 **(K)** mRNA expression of DCV following DmHSF1 overexpression post-DmAtta
1035 Knockdown. mRNA expression of DCV at high (30 °C) temperatures following
1036 DmHSF1 overexpression post-DmAtta knockdown. (k) Protein expression of DCV at
1037 high (30°C) temperatures following DmHSF1 overexpression post-DmAtta
1038 knockdown.
1039 Statistical significance was calculated using the Student's *t*-test (**$p < 0.01$, *$p < 0.05$).
1040 All experiments were conducted with three biological replicates, consistently yielding
1041 similar results.
1042

1043 **Figure 9.**

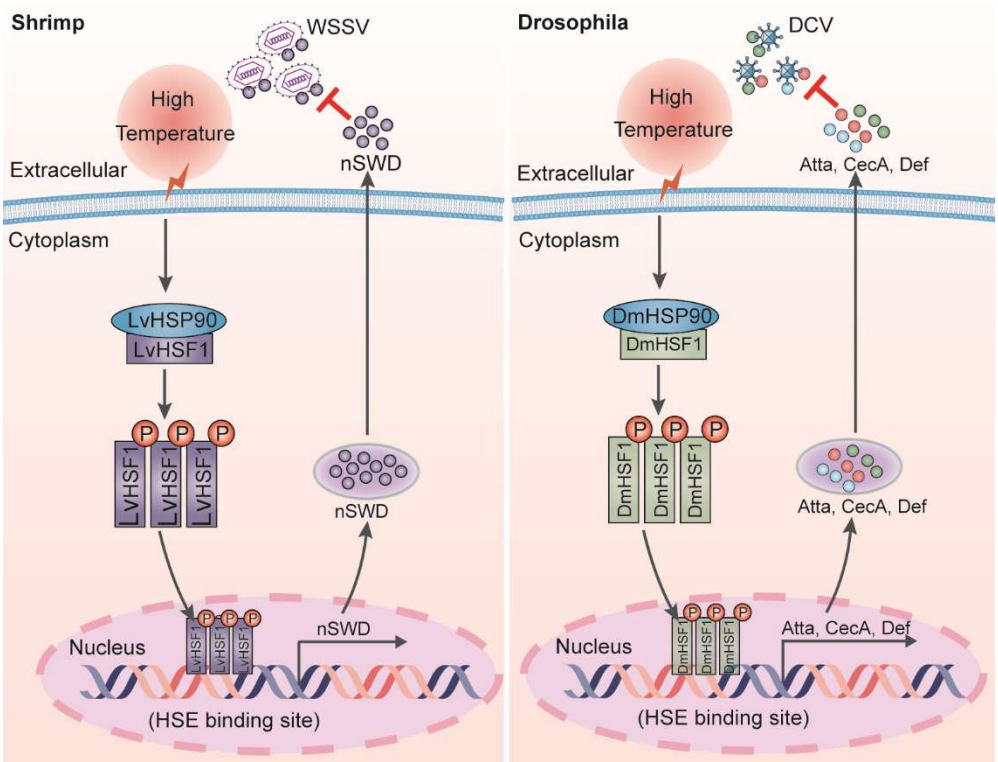

1044

1045 **Figure 9. Model for the HSF1-AMPs-mediated high temperature-induced**
1046 **resistance to viruses in arthropods.**

1047 Elevated temperature induces a robust expression of LvHSF1, which in turn specifically
1048 induces the expression of the antimicrobial peptide (SWD) in shrimp. The SWD
1049 directly binds to WSSV envelope proteins and inhibits WSSV replication (**left panel**).
1050 Additionally, elevated temperature induces the expression of DmHSF1, which
1051 upregulates the expression of Atta, CecA, and Def in *Drosophila* S2 cells, subsequently
1052 restricting the replication of DCV (**right panel**). These findings highlight the roles of
1053 HSF1 beyond the classical heat shock response, mediating the thermal regulation of
1054 immunity and facilitating the innate immune system's response against viruses.

1055

1056 **Supplementary Figure 1. The expression of transcription factors as determined by**
1057 **qPCR.**

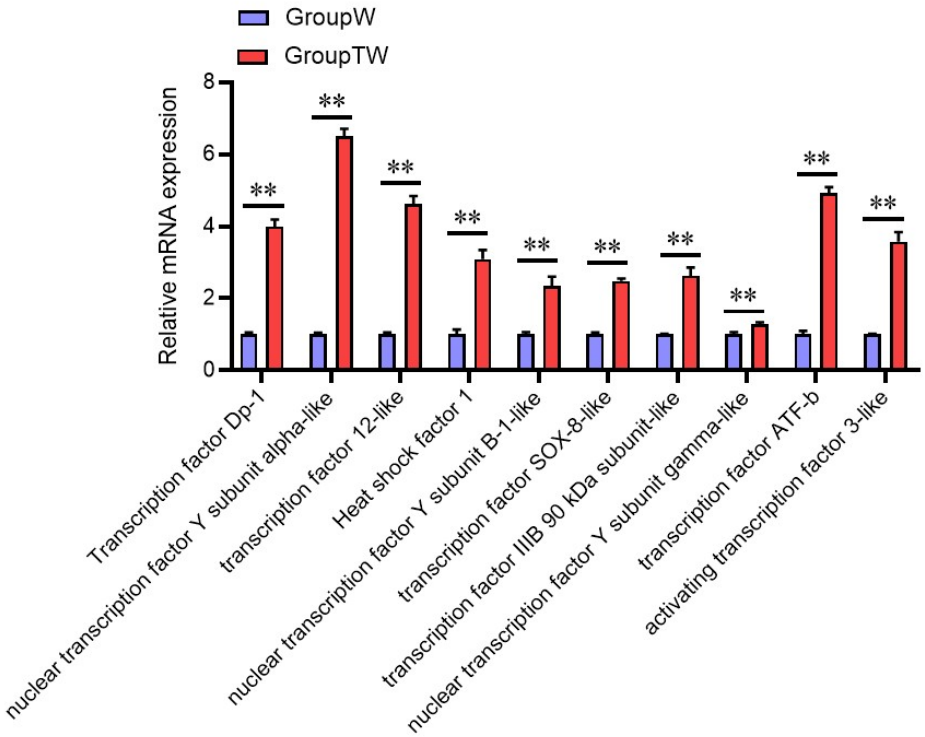

1058
1059

1060 **Supplementary Figure 2. The expression of profiles of LvHSF1 after Poly (I:C)**
1061 **injection at low temperature (25 °C).** (A-C) Expression profiles of LvHSF1 after Poly
1062 (I:C) injection at low temperatures (25 °C) in hemocytes (A), gills (B) and intestines
1063 (C). Expression levels were measured by qPCR, normalized against EF-1α and β-Actin
1064 using the Livak ($2^{-\Delta\Delta CT}$) method, and presented as mean ± SD from triplicate assays.
1065 (D-F) Expression profiles of LvHSF1 after WSSV injection at low temperatures (25 °C)
1066 in hemocytes (D), gills (E) and intestines (F). Expression levels were measured by
1067 qPCR, normalized against EF-1α and β-Actin using the Livak ($2^{-\Delta\Delta CT}$) method, and
1068 presented as mean ± SD from triplicate assays.
1069

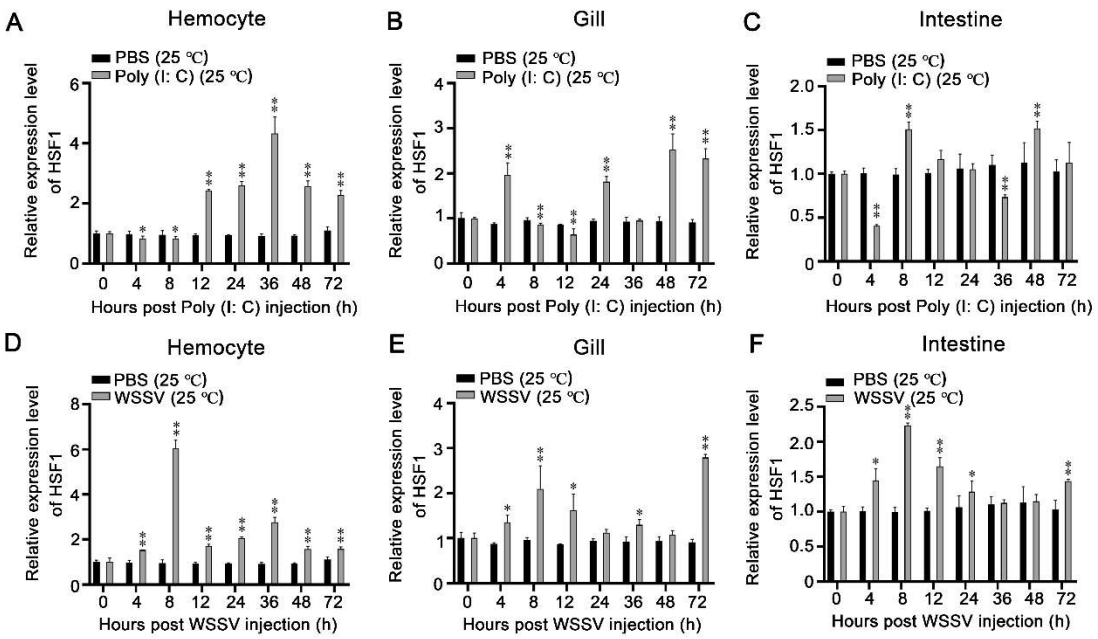

Supplementary Figure 3. SWD conserved sequence alignment in different shrimp species.

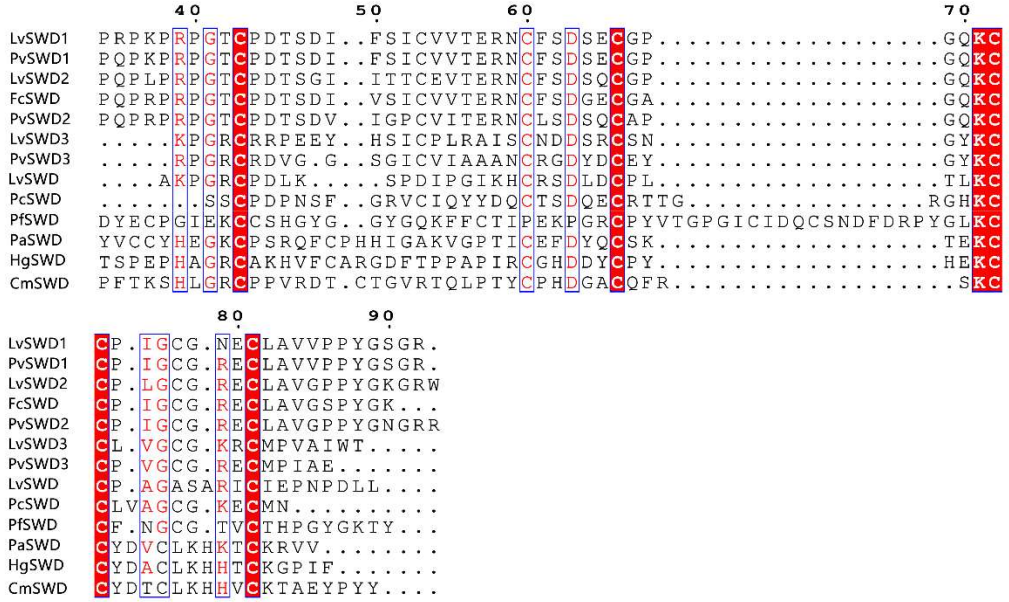

Supplementary Figure 4. The expression of effector molecules as determined by qPCR.

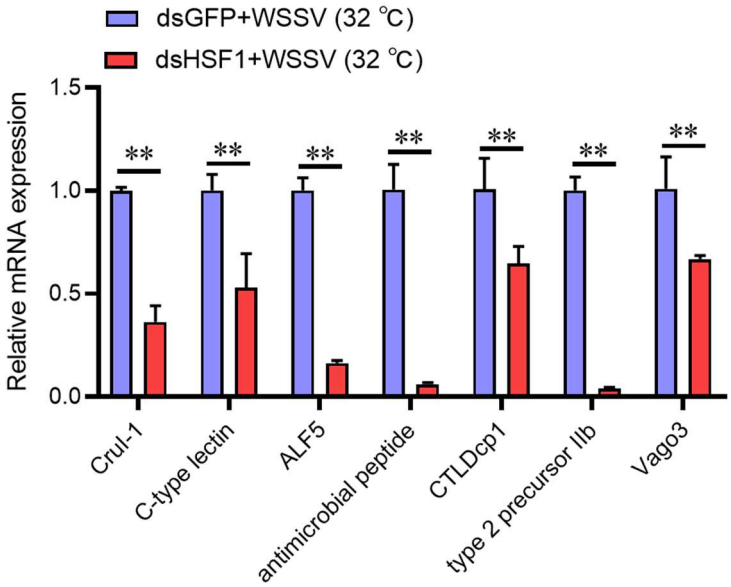

Supplementary Figure 5. SDS-PAGE and western blotting analyses of the recombinant LvHSF1 protein expressed in *E. coli*. (A) SDS-PAGE analysis of the recombinant LvHSF1 protein. Line 1, uninduced *E. coli* transformed with LvHSF1; line 2, induced *E. coli* transformed with LvHSF1; line 3, supernatant of ultrasonic lysed *E. coli* expressing LvHSF1; line 4, precipitate of lysed *E. coli* expressing LvHSF1; line 5, purified recombinant LvHSF1 protein (black arrow). (B) Western blotting analysis of the recombinant LvHSF1 protein. Line 1, rLvHSF1-GST; Line 2, GST (black arrow). Purified proteins were checked by Western blotting with anti-GST. (C) The expression of SWD after administration of GST or HSF1 protein in shrimp. (D) WSSV copy after knockdown SWD following injection with rLvHSF1 mixed with WSSV. Statistical significance was calculated using the Student's *t*-test (**$p < 0.01$, *$p < 0.05$). All experiments were conducted with three biological replicates, consistently yielding similar results.

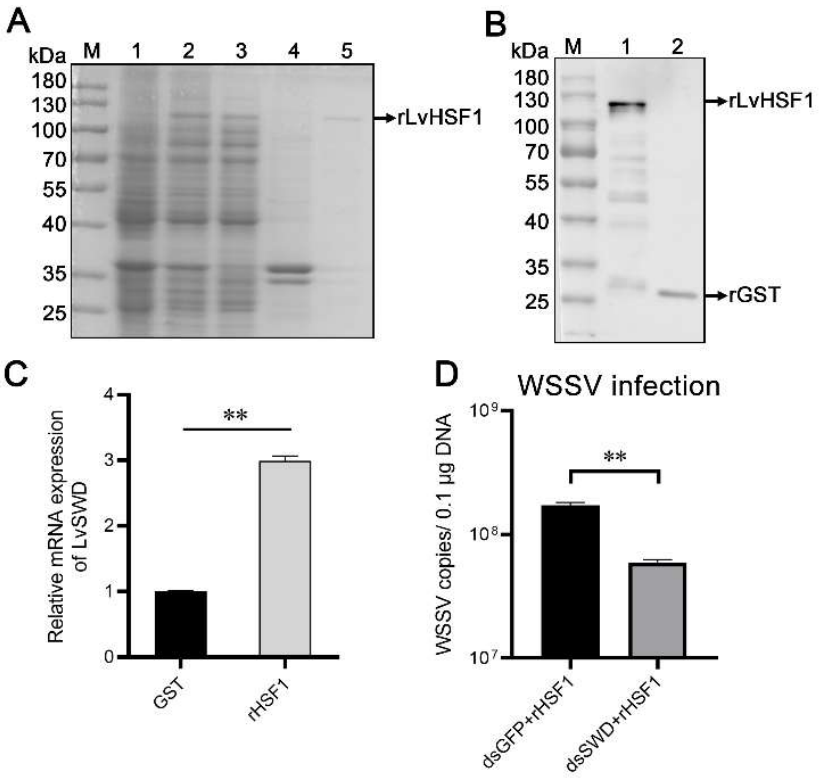

Supplementary Figure 6. High temperature restricts DCV replication in *Drosophila* S2 cells. (A) *Drosophila* S2 cells were seeded in 6-well plate and incubated at 27 ℃ or 30 ℃ for 24 h, then the cells were infected with DCV at a multiplicity of infection (MOI) of 10 at 27 ℃ or 30 ℃ for another 24 h. The cytopathic signs of S2 cells were observed in inverted fluorescence microscope. (B) The transcriptional expression of DCV in S2 cells with or without DCV infection (black arrow). (C) The protein expression of DCV in S2 cells with or without DCV infection.

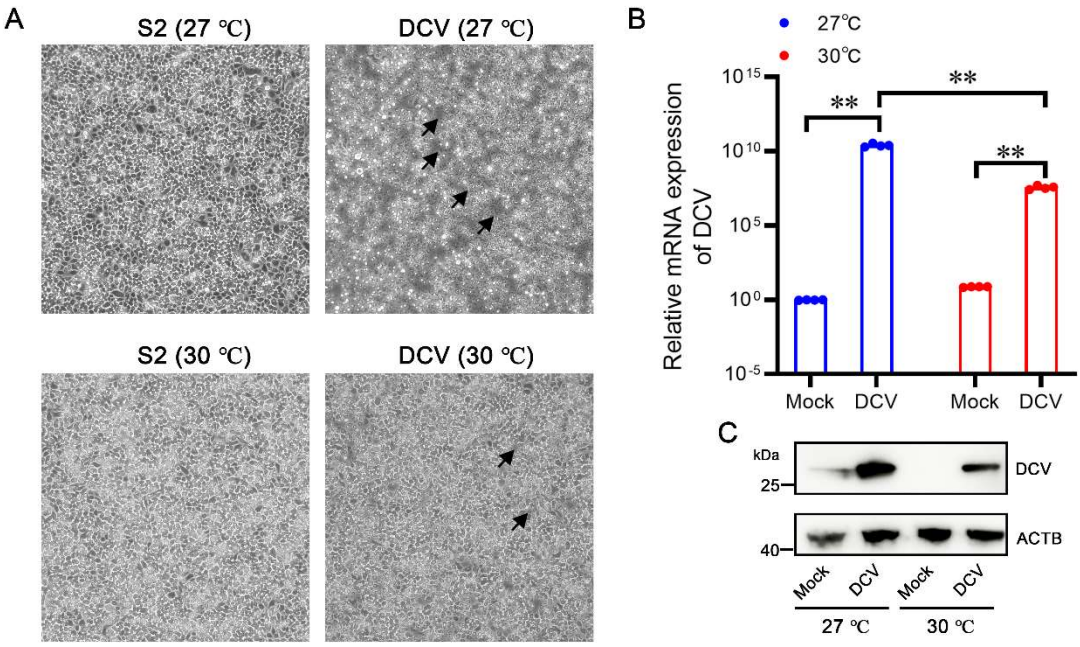

Supplementary Figure 7. Transfection in S2 cells. (A) The protein expression level of DmHSF1 was detected by western blotting at 48 h post-transfection in S2 cells. (B) The silencing efficiency of DmAtta in S2 cells 24 h after dsRNA application with or without DCV infection.

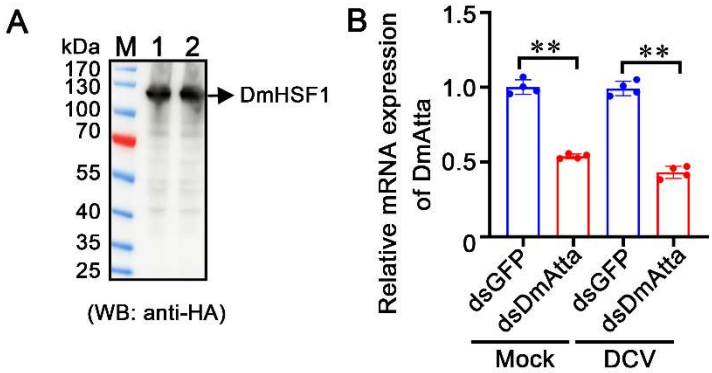

1111 **Reference**

1112 Akerfelt, M., Morimoto, R.I., Sistonen, L., 2010. Heat shock factors: integrators of cell stress,
1113 development and lifespan. *Nat Rev Mol Cell Biol* 11, 545-555.
1114 Akerfelt, M., Trouillet, D., Mezger, V., Sistonen, L., 2007. Heat shock factors at a crossroad between stress
1115 and development. *Ann N Y Acad Sci* 1113, 15-27.
1116 Amin, J., Ananthan, J., Voellmy, R., 1988. Key features of heat shock regulatory elements. *Mol Cell Biol*
1117 8, 3761-3769.
1118 Anckar, J., Sistonen, L., 2011. Regulation of HSF1 function in the heat stress response: implications in
1119 aging and disease. *Annu Rev Biochem* 80, 1089-1115.
1120 Andrasi, N., Pettko-Szandtner, A., Szabados, L., 2021. Diversity of plant heat shock factors: regulation,
1121 interactions, and functions. *J Exp Bot* 72, 1558-1575.
1122 Barna, J., Csermely, P., Vellai, T., 2018. Roles of heat shock factor 1 beyond the heat shock response. *Cell*
1123 *Mol Life Sci* 75, 2897-2916.
1124 Bicego, K.C., Barros, R.C.H., Branco, L.G.S., 2007. Physiology of temperature regulation: comparative
1125 aspects. *Comp Biochem Physiol A Mol Integr Physiol* 147, 616-639.
1126 Brogden, K.A., 2005. Antimicrobial peptides: pore formers or metabolic inhibitors in bacteria? *Nat Rev*
1127 *Microbiol* 3, 238-250.
1128 Bundey, S., Raymond, S., Dean, P., Roberts, S.K., Dillon, R.J., Charnley, A.K., 2003. Eicosanoid involvement
1129 in the regulation of behavioral fever in the desert locust, Schistocerca gregaria. *Arch Insect Biochem*
1130 *Physiol* 52, 183-192.
1131 Carpenter, S., O'Neill, L.A.J., 2024. From periphery to center stage: 50 years of advancements in innate
1132 immunity. *Cell* 187, 2030-2051.
1133 Casterlin, M.E., Reynolds, W.W., 1978. Prostaglandin E1 fever in the crayfish Cambarus bartoni.
1134 *Pharmacol Biochem Behav* 9, 593-595.
1135 Casterlin, M.E., Reynolds, W.W., 1979. Fever induced in marine arthropods by prostaglandin E1. *Life Sci*
1136 25, 1601-1603.
1137 Chen, J., Xie, C., Tian, L., Hong, L., Wu, X., Han, J., 2010. Participation of the p38 pathway in *Drosophila*
1138 host defense against pathogenic bacteria and fungi. *Proc Natl Acad Sci U S A* 107, 20774-20779.
1139 Covert, J.B., Reynolds, W.W., 1977. Survival value of fever in fish. *Nature* 267, 43-45.
1140 Deldicq, N., Langlet, D., Delaeter, C., Beaugrand, G., Seuront, L., Bouchet, V.M.P., 2021. Effects of
1141 temperature on the behaviour and metabolism of an intertidal foraminifera and consequences for
1142 benthic ecosystem functioning. *Sci Rep* 11, 4013.
1143 Du, H.H., Li, W.F., Xu, Z.R., Kil, Z.S., 2006. Effect of hyperthermia on the replication of white spot
1144 syndrome virus (WSSV) in *Procambarus clarkii*. *Dis Aquat Organ* 71, 175-178.
1145 Evans, S.S., Repasky, E.A., Fisher, D.T., 2015. Fever and the thermal regulation of immunity: the immune
1146 system feels the heat. *Nat Rev Immunol* 15, 335-349.
1147 Fan-xin, M., Li-mei, S., Bei, S., Xin, Q., Yu, Y., Yu, C., 2012. Heat shock factor 1 regulates the expression
1148 of the TRPV1 gene in the rat preoptic-anterior hypothalamus area during lipopolysaccharide-induced
1149 fever. *Exp Physiol* 97, 730-740.
1150 Filone, C.M., Caballero, I.S., Dower, K., Mendillo, M.L., Cowley, G.S., Santagata, S., Rozelle, D.K., Yen, J.,
1151 Rubins, K.H., Hacohen, N., Root, D.E., Hensley, L.E., Connor, J., 2014. The master regulator of the cellular
1152 stress response (HSF1) is critical for orthopoxvirus infection. *PLoS Pathog* 10, e1003904.
1153 Freitas Lione, V.O., Bittencourt Dos Santos, M.H., Ulisses Carvalho, T.M., Hirata, R., Jr., Mattos-Guaraldi,
1154 A.L., Arruda Mortara, R., Nagao, P.E., 2010. Fever temperature enhances mechanisms of survival of

1155 Streptococcus agalactiae within human endothelial cells. *Int J Mol Med* 26, 511-516.
1156 Fu, Q., Li, H., Wang, S., Liao, X., Chen, S., Xiao, B., Chen, R., Jiang, X., He, J., Li, C., 2022. An AhR-Caspase
1157 Axis Mediated Antiviral Apoptosis in an Arthropod. *J Immunol* 209, 2022-2032.
1158 Gao, J., Zhao, B.R., Zhang, H., You, Y.L., Li, F., Wang, X.W., 2021. Interferon functional analog activates
1159 antiviral Jak/Stat signaling through integrin in an arthropod. *Cell Rep* 36, 109761.
1160 Granja, C.B., Aranguren, L.F., Vidal, O.M., Aragon, L., Salazar, M., 2003. Does hyperthermia increase
1161 apoptosis in white spot syndrome virus (WSSV)-infected Litopenaeus vannamei? *Dis Aquat Organ* 54,
1162 73-78.
1163 Guan, Y., Yu, Z., Li, C., 2003. The effects of temperature on white spot syndrome infections in
1164 *Marsupenaeus japonicus*. *J Invertebr Pathol* 83, 257-260.
1165 Hasday, J.D., Singh, I.S., 2000. Fever and the heat shock response: distinct, partially overlapping
1166 processes. *Cell Stress Chaperones* 5, 471-480.
1167 Hasday, J.D., Thompson, C., Singh, I.S., 2014. Fever, immunity, and molecular adaptations. *Compr Physiol*
1168 4, 109-148.
1169 Hou, G., Lv, Z., Liu, W., Xiong, S., Zhang, Q., Li, C., Wang, X., Hu, L., Ding, C., Song, R., Wang, H., Zhang,
1170 Y.A., Xiao, T., Li, J., 2023. An aquatic virus exploits the IL6-STAT3-HSP90 signaling axis to promote viral
1171 entry. *PLoS Pathog* 19, e1011320.
1172 Jiravanichpaisal, P., Soderhall, K., Soderhall, I., 2004. Effect of water temperature on the immune
1173 response and infectivity pattern of white spot syndrome virus (WSSV) in freshwater crayfish. *Fish*
1174 *Shellfish Immunol* 17, 265-275.
1175 Kluger, M.J., Ringler, D.H., Anver, M.R., 1975. Fever and survival. *Science* 188, 166-168.
1176 Kumsta, C., Chang, J.T., Schmalz, J., Hansen, M., 2017. Hormetic heat stress and HSF-1 induce autophagy
1177 to improve survival and proteostasis in C. elegans. *Nat Commun* 8, 14337.
1178 Lang, B.J., Guerrero, M.E., Prince, T.L., Okusha, Y., Bonorino, C., Calderwood, S.K., 2021. The functions
1179 and regulation of heat shock proteins; key orchestrators of proteostasis and the heat shock response.
1180 *Arch Toxicol* 95, 1943-1970.
1181 Lee, H., Lee, S.V., 2022. Recent Progress in Regulation of Aging by Insulin/IGF-1 Signaling in
1182 Caenorhabditis elegans. *Mol Cells* 45, 763-770.
1183 Li, H., Di, X., Wang, S., Li, Q., Weng, S., He, J., Li, C., 2024. Nucleic Acid Sensing by STING Induces an IFN-
1184 like Antiviral Response in a Marine Invertebrate. *J Immunol* 212, 1945-1957.
1185 Li, H., Yin, B., Wang, S., Fu, Q., Xiao, B., Lu, K., He, J., Li, C., 2018. RNAi screening identifies a new Toll
1186 from shrimp *Litopenaeus vannamei* that restricts WSSV infection through activating Dorsal to induce
1187 antimicrobial peptides. *PLoS Pathog* 14, e1007109.
1188 Li, Z., Chen, W., Xu, L., Li, F., Yang, F., 2015. Identification of the interaction domains of white spot
1189 syndrome virus envelope proteins VP28 and VP24. *Virus Res* 200, 24-29.
1190 Lin, Y.R., Hung, H.C., Leu, J.H., Wang, H.C., Kou, G.H., Lo, C.F., 2011. The role of aldehyde dehydrogenase
1191 and hsp70 in suppression of white spot syndrome virus replication at high temperature. *J Virol* 85, 3517-
1192 3525.
1193 Liu, L.K., Jian, J.T., Jing, S.S., Gao, R.L., Chi, X.D., Tian, G., Liu, H.P., 2024. The crustacean DNA virus
1194 tegument protein VP26 binds to SNAP29 to inhibit SNARE complex assembly and autophagic
1195 degradation. *J Virol* 98, e0140823.
1196 Loh, E., Kugelberg, E., Tracy, A., Zhang, Q., Gollan, B., Ewles, H., Chalmers, R., Pelicic, V., Tang, C.M., 2013.
1197 Temperature triggers immune evasion by Neisseria meningitidis. *Nature* 502, 237-240.
1198 Louis, C., Jourdan, M., Cabanac, M., 1986. Behavioral fever and therapy in a rickettsia-infected

1199 Orthoptera. *Am J Physiol* 250, R991-995.
1200 M.E. Casterlin, W.W.R., 1977. Bahavioral fever in crayfish. *Hydrobiologia* 56, 99-101.
1201 Marcogliese, D.J., 2008. The impact of climate change on the parasites and infectious diseases of aquatic
1202 animals. *Rev Sci Tech* 27, 467-484.
1203 Matos, G.M., Rosa, R.D., 2022. On the silver jubilee of crustacean antimicrobial peptides. *Rev Aquacult*
1204 14, 594-612.
1205 Merkling, S.H., Overheul, G.J., van Mierlo, J.T., Arends, D., Gilissen, C., van Rij, R.P., 2015. The heat shock
1206 response restricts virus infection in *Drosophila*. *Sci Rep* 5, 12758.
1207 Methatham, T., Boonchuen, P., Jaree, P., Tassanakajon, A., Somboonwiwat, K., 2017. Antiviral action of
1208 the antimicrobial peptide ALFPm3 from *Penaeus monodon* against white spot syndrome virus. *Dev*
1209 *Comp Immunol* 69, 23-32.
1210 Millard, R.S., Ellis, R.P., Bateman, K.S., Bickley, L.K., Tyler, C.R., van Aerle, R., Santos, E.M., 2021. How do
1211 abiotic environmental conditions influence shrimp susceptibility to disease? A critical analysis focussed
1212 on White Spot Disease. *J Invertebr Pathol* 186, 107369.
1213 Morano, K.A., Grant, C.M., Moye-Rowley, W.S., 2012. The response to heat shock and oxidative stress
1214 in Saccharomyces cerevisiae. *Genetics* 190, 1157-1195.
1215 Morimoto, R.I., 2011. The heat shock response: systems biology of proteotoxic stress in aging and
1216 disease. *Cold Spring Harb Symp Quant Biol* 76, 91-99.
1217 Neef, D.W., Jaeger, A.M., Gomez-Pastor, R., Willmund, F., Frydman, J., Thiele, D.J., 2014. A direct
1218 regulatory interaction between chaperonin TRiC and stress-responsive transcription factor HSF1. *Cell*
1219 *Rep* 9, 955-966.
1220 Nekongo, E.E., Ponomarenko, A.I., Dewal, M.B., Butty, V.L., Browne, E.P., Shoulders, M.D., 2020. HSF1
1221 Activation Can Restrict HIV Replication. *ACS Infect Dis* 6, 1659-1666.
1222 Niu, G.J., Wang, S., Xu, J.D., Yang, M.C., Sun, J.J., He, Z.H., Zhao, X.F., Wang, J.X., 2019. The polymeric
1223 immunoglobulin receptor-like protein from *Marsupenaeus japonicus* is a receptor for white spot
1224 syndrome virus infection. *PLoS Pathog* 15, e1007558.
1225 Pan, X.Y., Zhao, W., Zeng, X.Y., Lin, J., Li, M.M., Shen, X.T., Liu, S.W., 2016. Heat Shock Factor 1 Mediates
1226 Latent HIV Reactivation. *Sci Rep* 6, 26294.
1227 Rahman, M.M., Corteel, M., Wille, M., Alday-Sanz, V., Pensaert, M.B., Sorgeloos, P., Nauwynck, H.J.,
1228 2007. The effect of raising water temperature to 33 °C in *Penaeus vannamei* juveniles at different stages
1229 of infection with white spot syndrome virus (WSSV). *Aquaculture* 272, 240-245.
1230 Rakhshaninejad, M., Zheng, L., Nauwynck, H., 2023. Shrimp (*Penaeus vannamei*) survive white spot
1231 syndrome virus infection by behavioral fever. *Sci Rep* 13, 18034.
1232 Rakus, K., Ronsmans, M., Forlenza, M., Boutier, M., Piazzon, M.C., Jazowiecka-Rakus, J., Gatherer, D.,
1233 Athanasiadis, A., Farnir, F., Davison, A.J., Boudinot, P., Michiels, T., Wiegertjes, G.F., Vanderplasschen, A.,
1234 2017. Conserved Fever Pathways across Vertebrates: A Herpesvirus Expressed Decoy TNF-alpha
1235 Receptor Delays Behavioral Fever in Fish. *Cell Host Microbe* 21, 244-253.
1236 Reyes, A., Navarro, A.J., Diethelm-Varela, B., Kalergis, A.M., Gonzalez, P.A., 2022. Is there a role for HSF1
1237 in viral infections? *FEBS Open Bio* 12, 1112-1124.
1238 Singh, V., Aballay, A., 2006. Heat-shock transcription factor (HSF)-1 pathway required for Caenorhabditis
1239 elegans immunity. *Proc Natl Acad Sci U S A* 103, 13092-13097.
1240 Sun, Y., Li, F., Sun, Z., Zhang, X., Li, S., Zhang, C., Xiang, J., 2014. Transcriptome analysis of the initial stage
1241 of acute WSSV infection caused by temperature change. *PLoS One* 9, e90732.
1242 Tian, F., Hu, X.L., Yao, T., Yang, X., Chen, J.G., Lu, M.Z., Zhang, J., 2021. Recent Advances in the Roles of

1243 HSFs and HSPs in Heat Stress Response in Woody Plants. *Front Plant Sci* 12, 704905.
1244 Vatanavicharn, T., Supungul, P., Puanglarp, N., Yingvilasprasert, W., Tassanakajon, A., 2009. Genomic
1245 structure, expression pattern and functional characterization of crustinPm5, a unique isoform of crustin
1246 from *Penaeus monodon*. *Comp Biochem Physiol B Biochem Mol Biol* 153, 244-252.
1247 Wang, S., Li, H., Weng, S., Li, C., He, J., 2020. White Spot Syndrome Virus Establishes a Novel IE1/JNK/c-
1248 Jun Positive Feedback Loop to Drive Replication. iScience 23, 100752.
1249 Wang, S., Sun, Y., Wang, Y., Wang, A., Kou, B., Che, Y., Chen, D., Zhang, Y., Shi, Y., 2021. ASPP2 inhibits
1250 hepatitis B virus replication by preventing nucleus translocation of HSF1 and attenuating the
1251 transactivation of ATG7. *J Cell Mol Med* 25, 6899-6908.
1252 Wang, X.X., Zhang, H., Gao, J., Wang, X.W., 2024. Ammonia stress-induced heat shock factor 1 enhances
1253 white spot syndrome virus infection by targeting the interferon-like system in shrimp. *mBio* 15,
1254 e0313623.
1255 Weihrauch, D., Joseph, G., Allen, G.J.P., 2018. Ammonia excretion in aquatic invertebrates: new insights
1256 and questions. *J Exp Biol* 221.
1257 Wu, X., Xiong, H., Wang, Y., Du, H., 2015. Immunomodulatory effects of hyperthermia on resisting WSSV
1258 infection in Procambarus clarkii. *J Fish Dis* 38, 567-574.
1259 Xiao, B., Fu, Q., Niu, S., Zhu, P., He, J., Li, C., 2020. Penaeidins restrict white spot syndrome virus infection
1260 by antagonizing the envelope proteins to block viral entry. *Emerg Microbes Infect* 9, 390-412.
1261 Xiao, B., Liao, X., Wang, H., He, J., Li, C., 2021. BigPEN, an antimicrobial peptide of penaeidin family from
1262 shrimp Litopenaeus vannamei with membrane permeable and DNA binding activity. *Fish Shellfish*
1263 *Immunol Rep* 2, 100034.
1264 Xiao, B., Wang, Y., He, J., Li, C., 2024. Febrile Temperature Acts through HSP70-Toll4 Signaling to Improve
1265 Shrimp Resistance to White Spot Syndrome Virus. *J Immunol* 213, 1187-1201.
1266 Xiao, H., Lis, J.T., 1988. Germline transformation used to define key features of heat-shock response
1267 elements. *Science* 239, 1139-1142.
1268 Yang, S., Yu, J., Fan, Z., Gong, S.T., Tang, H., Pan, L., 2018. Bub1 Facilitates Virus Entry through Endocytosis
1269 in a Model of *Drosophila* Pathogenesis. *J Virol* 92.
1270 You, X.X., Su, Y.Q., Mao, Y., Liu, M., Wang, J., Zhang, M., Wu, C., 2010. Effect of high water temperature
1271 on mortality, immune response and viral replication of WSSV-infected juveniles and adults. *Aquaculture*
1272 305, 133-137.
1273 Yuasa, K., Ito, T., Sano, M., 2008. Effect of Water Temperature on Mortality and Virus Shedding in Carp
1274 Experimentally Infected with Koi Herpesvirus. *Fish Pathol* 43, 83-85.
1275 Zhang, X., Yuan, J., Sun, Y., Li, S., Gao, Y., Yu, Y., Liu, C., Wang, Q., Lv, X., Zhang, X., Ma, K.Y., Wang, X., Lin,
1276 W., Wang, L., Zhu, X., Zhang, C., Zhang, J., Jin, S., Yu, K., Kong, J., Xu, P., Chen, J., Zhang, H., Sorgeloos, P.,
1277 Sagi, A., Alcivar-Warren, A., Liu, Z., Wang, L., Ruan, J., Chu, K.H., Liu, B., Li, F., Xiang, J., 2019. Penaeid
1278 shrimp genome provides insights into benthic adaptation and frequent molting. *Nat Commun* 10, 356.
1279 Zhao, Z.Y., Yin, Z.X., Xu, X.P., Weng, S.P., Rao, X.Y., Dai, Z.X., Luo, Y.W., Yang, G., Li, Z.S., Guan, H.J., Li, S.D.,
1280 Chan, S.M., Yu, X.Q., He, J.G., 2009. A novel C-type lectin from the shrimp Litopenaeus vannamei
1281 possesses anti-white spot syndrome virus activity. *Journal of Virology* 83, 347-356.
1282 Zheng, X., Krakowiak, J., Patel, N., Beyzavi, A., Ezike, J., Khalil, A.S., Pincus, D., 2016. Dynamic control of
1283 Hsf1 during heat shock by a chaperone switch and phosphorylation. *Elife* 5.
1284 Zhu, F., Ding, H., Zhu, B., 2013. Transcriptional profiling of *Drosophila* S2 cells in early response to
1285 *Drosophila* C virus. *Virol J* 10, 210.
1286